Subcritical and Supercritical CO$_2$ Adsorption Capacity of Post-UCG Gasified Coal

by

Sara Zabihi

A thesis submitted in partial fulfillment of the requirements for the degree of

Master of Science

in

Petroleum Engineering

Department of Civil and Environmental Engineering
University of Alberta

Abstract

Because of the increasing curiosity in the effectiveness of Underground Coal Gasification-Carbon Capturing and Storage (UCG-CCS) sites for carbon sequestration, an urge for a new line of research has emerged to measure the amount of CO2 adsorption in gasified coal as a potential long-term solution for global warming.

In this study, the adsorption capacities of gasified coal from a UCG experiment is measured using a volumetric adsorption apparatus at 45.5 ℃ and 500 Psia to 1500 Psia, and CO_2 adsorption isotherms are obtained. This pressure range was chosen to cover both sub and super critical pressure regions of CO_2. Additionally, the effect of the UCG process on surface area and pore volume development was investigated to correlate them to the adsorption capacity of the samples. The results indicate that the adsorption amount of the gasified coals increases as the pressure rises in the system, and continues to increase with a sharper slope after it passed the critical pressure of CO_2. It was also observed that the surface area and pore volume of the samples increase more than two times during the gasification process, and up to 65 percent of the fixed carbon content in the samples converts to syngas. Samples farther from the ignition channel in UCG showed more conversion and structure transformation. The adsorption capacities of samples increased linearly with surface area and pore volume increments. The pore size distribution illustrated that pores with 1.5 nm in diameter contributed most effectively to the surface area of the samples. In addition, the SEM images of the gasified and raw coals validated the pore structure development due to the gasification.

Keywords: CO_2 adsorption on coal, UCG-CCS, underground coal gasification-carbon capturing and storage, volumetric apparatus, gasified coal adsorption capacity

Preface

The gasified coal samples for adsorption measurement in this research came from the UCG experiments conducted by Monir Khan at the University of Alberta for his PhD work focusing on the cavity modeling of the UCG process.

The volumetric adsorption apparatus used for adsorption measurement in this work is from the M.Sc. work of Pavan Pramod Sripada who carried out the CO_2 adsorption capacities of raw and pyrolyzed coal.

Volumetric adsorption sample preparation, all adsorption measurement experiments, BET and TGA experiments, SEM images and analyses, and data analyses presented in this thesis are independent work done by the author, Sara Zabihi.

Acknowledgements

I would first like to thank my thesis advisors Dr. Japan Trivedi and Professor Rajender Gupta at University of Alberta. The door to their office was always open whenever I ran into a trouble spot or had a question about my research. They have always been a source of great inspiration, encouragement, guidance, and support.

Special thanks to Monir Khan and Dr. Deepak Pudasainee for helping me finding my way at the beginning of my research and teaching me how to work with different apparatuses. I would also take the opportunity to thank Todd Kinnee at the school of Petroleum Engineering for helping rearrange my experimental setup and ensure the safety of the apparatus.

I had the opportunity to work with Dr. Mehdi Alipour and Ni Yang for the SEM images of my samples. They generously took the time to help me and I am so grateful for their support. Thanks Professor Zaher Hashisho for agreeing to be a part of my exam committee with a short notice.

The funding support from the coal mining research company as a graduate scholarship is also gratefully acknowledged.

Finally, Thanks to my parents for their infinite support and encouragement. I must express my very profound gratitude to my husband, Dr. Mohammad Feizbakhshan, for providing me with unfailing support and continuous encouragement throughout my years of study and through the process of researching and writing this thesis. This accomplishment would not have been possible without him. Thank you.

Table of Contents

vi

List of Figures

List of Tables

Acronyms

CCS   Carbon Capturing and Storage

DOE   US Department of Energy

DTG   Derivative Thermogravimetric Analysis

UCG   Underground Coal Gasification

IUPAC   International Union of Pure and Applied Chemistry

SEM   Scanning Electron Microscopy

TGA   Thermogravimetric Analysis

UCG-CCS   Underground Coal Gasification- Carbon Capturing and Storage

Chapter 1

1 Introduction

1.1 General introduction

The amount of carbon dioxide emitted to the atmosphere due to human activities has ascended from the preindustrial level of 280 ppm to the current level of 401 ppm (1, 2). According to the U.S. Department of Energy (DOE), one way of carbon management is to alternate lower-carbon or carbon-free energy sources with the ongoing conventional sources. For example, substituting lower carbon fossil fuels like natural gas for coal or oil might be considered. Another approach is carbon sequestration, which includes both natural and deliberate processes for managing carbon emission. In this method, natural and anthropogenic CO_2 is either cleared away from the atmosphere or captured at its emission sources and stored at riskless sites. Approximately 85 to 90 percent of carbon dioxide to be emitted to the atmosphere, could be managed for capture and storage through a CCS (Carbon capturing and storage) strategy.

Nowadays, Underground coal gasification (UCG) is a proven technology because of its plentiful advantages over conventional underground strip mining and surface gasification. UCG has gained a significant added advantage over alternative clean coal technologies since the gasified cavity, which is left after the gasification process, can be an economically efficient storage zone for the greenhouse gas emission (3). Moreover, UCG-CCS incorporates both strategies of using cleaner energy sources and storing captured emissions in safe sites (4, 5).

1

It is necessary to learn the fundamentals of CO_2 storage in post-UCG sites for a better understanding of the UCG-CCS concept. Adsorption is the essential storing mechanism of carbon dioxide in coal beds at high pressures (6). According to Goodman et al, the interaction between the molecules of carbon dioxide and coal represents a physical adsorption known as physisorption (7). In physisorption, Van der Wall's bonds exist between the molecules of adsorbate and adsorbent, which can accommodate multiple layers of adsorbate molecules on the surface of the adsorbent. This phenomenon is termed as multi-layer adsorption (8, 9).

In the case of UCG-CCS, adsorption measurements and analysis are required for an adsorbent including dry coal, pyrolyzed coal, and partially gasified coal. Adsorption capacity of various raw coals are measured and reported in the literature (10-13). Experiments have also been conducted on CO_2 adsorption onto synthetically prepared pyrolyzed coal, in which the samples were pyrolyzed in a furnace at 700 °C to 1000 °C under an inert atmosphere (14). However, since samples in the experiments have not been prepared considering the operational conditions of UCG sites (using oxidants for gasification and allow pyrolysis and gasification occur naturally), it creates a challenging gap in the adsorption capacity measurement of the gasified coal, which needs to be alleviated.

In this study, the adsorption capacity of the partially gasified coal and naturally pyrolyzed coal is measured using a volumetric setup in laboratory. The coal samples are Canadian sub-bituminous coal which have been under the UCG experiment at the University of Alberta, the adsorption capacity of these samples is measured at 45.5 °C and pressures up to 1000 Psia in steps of 100 Psia. Moreover, for further analysis and the confirmation of the result, the surface area and pore volume of the samples, illustrative of the relations between adsorption capacity and available space for molecules to adhere, are measured using surface analyzer apparatus.

1.2 Hypotheses and objectives

In this research, the broad objective is to understand the suitability of remained coal from post UCG sites for underground geological CO_2 storage. UCG-CCS as a potential and economical CO_2 sequestration storage place has been a popular topic in the past decade. Some of the challenges are the abandoned UCG site's pressure and temperature, risk of stored gas leakage, storage capacity of remained coal, etc. Several researchers all over the world have worked on the adsorption capacity of raw coal and parameters affecting its capacity, as well as adsorption investigations on synthetically prepared gasified and pyrolyzed coal with exposure to high temperature and different gases such as nitrogen. However, samples from post UCG sites were not available to urge a study on their adsorption capacity. Thanks to the UCG process modelling apparatus at the University of Alberta, which takes Canadian sub-bituminous coal as feed, the opportunity to investigate post UCG site for potential CO_2 storage is provided. This research aims to answer the following questions:

1. Is the adsorption of CO_2 on gasified coal physisorption or chemisorption?

2. How does the pore volume and surface area of coal change during the gasification?

3. How does the pore size distribution of the coal samples change after the gasification?

4. What is the adsorption capacity of post-UCG gasified coal and how does it vary with pressure?

5. How does supercritical pressures of injecting CO_2 onto gasified coal affect the adsorption capacity?

6. What is the relationship of pore volume and surface area of the gasified samples with their adsorption capacity?

7. How does the distance of coal to the ignition channel in the gasification process affect the storage capacity in coal?

8. What is the effect of equilibrium time on adsorption value of the coal?

9. What is the contribution of pores developed by fixed carbon conversion in adsorption capacity of coal?

To answer these questions and to address some of the gaps in this area the adsorption capacity of post UCG gasified coals at underground temperature and high CO_2 injecting pressures including super critical pressures are measured. In addition to that, the influence of coal components, pore volume, pore size distribution, and surface area on the adsorption capacity of coal is investigated through different characterization tests.

1.3 Outlines

Chapter 2 summarizes basics in UCG and CCS concepts and reviews some of the works that have been done to capture the effect of influencing parameters along with a brief presentation of the techniques adopted for porosity, surface area, and adsorption measurements. Recent studies on pyrolyzed coal are also mentioned to demonstrate the need for this research.

Chapter 3 is all about experimental procedures that have been employed in this research such as UCG process coal block preparation, post UCG gasified coal sample preparation, volumetric adsorption setup instruction and specifications, two different TGA apparatus specifications and experiment procedure, and finally Surface analyzer apparatus specifications and experiments agenda.

Chapter 4 brings together the results of this study. It starts with coal characterization results from TGA. Gasified coal samples and adsorbed coal samples were tested to give proximate analysis and mass loss graph during heating process for comparison. Then surface analyzer apparatus outputs are discussed and atmospheric adsorption isotherm is presented. Volumetric adsorption results at pressure range of 500 Psia and 1000 Psia together with supercritical experiments outcome are presented and discussed.

Chapter 5 gives an overall conclusion of this work and recommends areas to work on for possible future studies.

Chapter 2

2 Literature Review

Coal is a fundamental ingredient of steel production and plays a critical role in electricity generation known as coal-fired power plants across the world. Both major industries (electricity generation out of fossil fuel and steel production for manufacturing) are leading CO_2 emitting sectors these days. Steel production emits carbon dioxide both in energy generating stage and during chemical reaction in the production process (15). Steel production has doubled over the last 35 years and continues to increase drastically. Carbon capturing and storage (CCS) solution to manage and control emission to atmosphere is shown to reduce 0.5-1.5 gigatonne of potential CO_2 from steel making industry per year and a total of 85 to 90 percent of all CO_2 emissions to the atmosphere. (5, 15).

2.1   UCG-CCS

Underground coal gasification is a process in which non-exploitable coal reserve, due to complex geology and un accessible depth, are directly converted to syngas for fuel and chemical use through in situ combustion (16).

This nearly new method of coal use is acknowledged to bring coal mining and surface combustion an environmentally conscious alternative (17). Figure 1 shows a schematic of underground coal gasification process. To simplify the process, UCG works as follows:

1.   A vertical injection well and a production well are drilled into the coal bed. These two vertical wells are linked together horizontally to allow for gas flow.

2. Ignition is required to spark the gasification process. In order to continue the combustion to reach self-burning state of coal, oxidant and steam are injected into the injection well.

3. During gasification, so many different reactions happen among which water gas shift reaction is the most important because it yields H_2 and CO known as syngas. Table 1 summarizes all main reactions occurring during gasification of coal (18).

4. Syngas travels to the production well through horizontal link provided between the two wells and goes up to surface. (3)

Figure 1 UCG Process and its cavity-Picture from linc energy (3)

Table 1 Chemical reactions during UCG (3)

	Reaction	Enthalpy
1	Heterogeneous water gas shift reaction $C+H_2O=H_2+CO$	$\Delta H = +118.5\ kJ\ mol^{-1}$
2	Shift Conversion $CO+H_2O= H_2+CO_2$	$\Delta H\ \ 42.3\ kJ\ mol^{-1}$
3	Methanation $CO+3H_2=CH_4+ H_2O$	$\Delta H =\ 206.0\ kJ\ mol^{-1}$
4	Hydrogenation gasification $C+2H_2=CH_4$	$\Delta H =\ 87.5\ kJ\ mol^{-1}$
5	Partial oxidation $C+1/2O_2= CO$	$\Delta H =\ 123.1\ kJ\ mol^{-1}$

6	Oxidation	$\Delta H = \ -406.0 \ kJ \ mol^{-1}$
	$C+O_2= CO_2$	
7	Boudouard reaction	$\Delta H = +159.9 \ kJ \ mol^{-1}$
	$C+ CO_2=2CO$	

Composition of the produced gas is not always the same. It depends upon the coal type, operating pressure, operating temperature, and the type of oxidant used (air or oxygen).

Simultaneous changes in underground rock stress field occurs while UCG process passes through the coal seam. Pore pressures, temperature, and buoyancy gradient as well as fracture's opening varies as a result of gasification process which alters the hydrologic flow path underground. Newly opened fracture and pore spaces provide the opportunity for old minerals to dissolve or new minerals to form, reshaping permeability of the rock (3). In the UCG cavity itself, pore sizes increase and new pores form, which leaves more storage capacity for further adsorption (19). Accordingly, the UCG process is incorporated with CCS to store CO_2 into the residual and newly formed voids, as well as adjacent coal seams in UCG process (20, 21).

Even though UCG-CCS is an economically and environmentally beneficial plan from sustainability viewpoints, there are a few challenges and uncertainties to be investigated. The operating conditions of post UCG sites such as pressure and temperature, the geo mechanic response of the reservoir, the risk of underground water table pollution, the adsorption capacity of the remained coal, and the supercritical adsorption values of CO_2 onto coal (which is not reported anywhere yet) are some of the challenges to be alleviated (3).

Because the temperature rises up to 1000 °C during UCG, it is necessary to monitor the temperature of post UCG site. To avoid CO_2 expansion due to temperature difference, cavity must be cooled down to retain the capacity for storage (16, 22). Cooling down could happen

naturally or by flushing water through UCG wells (22, 23). Given the underground water risk, attention is required to focus on preventing the leak of UCG byproducts such as tars, phenol, and benzene to the adjacent aquifers. Another risk involved in UCG-CCS project is CO_2 displacement that refers to the tendency of CO_2 to move toward cap rocks due to the changes in the effective stress of geological formation underground (16, 23). Plants, human, and animals are in danger of thoughtless CO_2 storage underground (3). The optimization of the operating conditions is of importance after the feasibility of CO_2 storage at available cavity depth has been studied for permanent carbon sequestration. The volume required to store CO_2 emitting from the UCG process itself is 4 to 5 times more than the available space due to coal extraction and gasification (23) that necessitate optimization of pressure and temperature at which the CO_2 is storing.

2.2 Storing mechanism of CO_2 onto coal

2.2.1 History of adsorption

Adsorption is the essential mechanism of carbon dioxide storage onto coal at high pressures (6). Back in 1777, Fontana realized that a porous solid such as charcoal could accommodate various gases up to several times of its own volume. Soon after it was figured out that, the void volume available to hold gas in a porous solid depends on the type of the gas and the solid. More specifically, the efficiency of the solid to hold gas in itself is relied upon the area of exposed solid surface to gas. Moreover, Mitscherlich, in 1843, brought up the importance of charcoal pore size and their average diameter as a dependent factor of gas volume adsorption capacity in a solid. Therefore, surface area and porosity or pore volume are now acknowledged to be integral parts of adsorption phenomena of all solids. Kayser first introduced the term

9

"adsorption" in 1881 to imply the condensation of a gas on a solid surface. Gaseous absorption on the other hand happens when gaseous molecules penetrate into the bulk of the solid. In an adsorption experiment, the solid, which adsorbs on its surface, is called "adsorbent" and the material adsorbed by solid is termed as "adsorbate". There are interacting forces between the solid and gas molecules, which cause adsorption. Adsorption could be either physical (physisorption) with the same nature of forces as Van der Waals or chemical (chemisorption).

There are more technical definitions for adsorption as an example of which, adsorption is defined as a process in which a molecule becomes adsorbed onto a surface of another phase. In other words, in a closed space filled with a solid and some gas, the solid such as charcoal starts to adsorb gas and gain weight by decreasing the pressure of the gas. This process is not unlimited and stops at a point with a constant pressure value. Incorporating gas pressure decrease amount into the gas law will give the adsorption value of gas (24-30)

2.2.2   Parameters affecting adsorption capacity

Factors affecting the quantity of gas that a solid can hold are mass of the sample, temperature, pressure of the gas and the nature of both adsorbent and adsorbate. Quantity of adsorbed gas as a function of its dependents can be written as follows:

$$n = f(P, T, Solid, gas) \qquad (2.1)$$

n: mole of adsorbed gas per gram of solid

The equation above (2.1) can be simplified to the equation below (2.2) for a specific gas on a particular solid if the temperature is kept constant:

$$n = f(P)_{T,\text{Solid,gas}} \quad (2.2)$$

It is more conventional to take the saturation vapor pressure of the adsorbate into the equation if the temperature is below the critical temperature of the gas:

$$n = f(P/P^0)_{T,\text{Solid,gas}} \quad (2.3)$$

P^0 is the saturation vapor pressure of the adsorbate gas.

Adsorption isotherms and their different types are discussed in the next section.

2.2.3   Adsorption Isotherms

The relationship between the amount of gas adsorbed at a constant temperature and the pressure or the relative pressure is known as the adsorption isotherm (24).
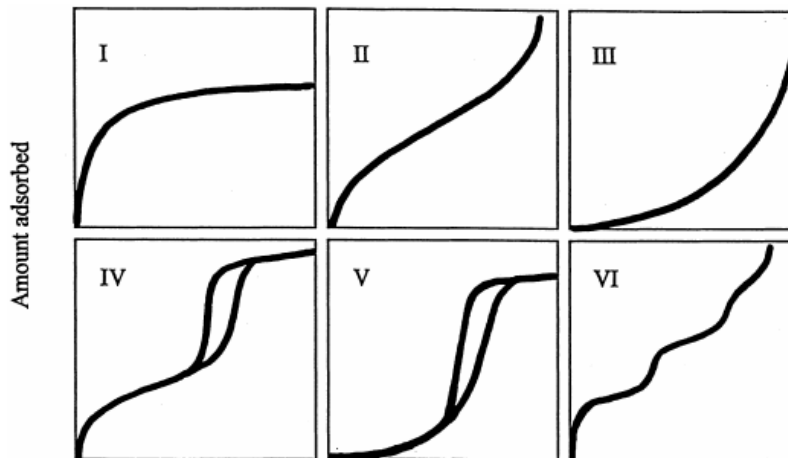
Figure 2 Different types of adsorption isotherm from BET (24)

Adsorption isotherm of more than ten thousand different solids and gases are recorded in the literature. Brunauer, Deming, Deming and Teller (BDDT) also known as Brunauer, Emmett and Teller (BET) grouped almost all physical adsorptions into five different classifications, which are known as the adsorption isotherm type. However, there are also a noticeable number

of other adsorption isotherms, which either cannot fit into these classifications or are difficult to assign to one of these five groups. Figure 2 shows the five essential types of isotherm proposed by BET (31).

2.2.4 Langmuir theory

Langmuir first presented a comprehensive theory of adsorption onto a flat surface in 1918. The theory was based on a kinetic viewpoint stating that bombardment of molecules onto the adsorbent surface and corresponding evaporation of molecules from the surface, termed as desorption, occurs incessantly to maintain the zero accumulation on the surface for equilibrium. There are a number of assumptions for this theory, which are summarized below:

1. Surface of the adsorbent is homogeneous which necessitate constant adsorption energy over all sites.

2. Adsorption on surface is localized; adsorbed atoms and molecules are adsorbed at definite localized sites.

3. Each site of adsorption only holds one molecule or atom.

2.2.5 Multilayer adsorption

An adsorbed molecule interacts both with the surface of the solid and with other molecules within the layer. The effect of interaction with other adsorbate molecules is not noticeable as long as there are not too many of them on a surface. Once it gets crowded on the layer, interaction of adsorbate molecules helps attract more molecules of gas, which results in multilayer adsorption built up.

The surface area of a given amount of solid is inversely related to the size of the solid particles. It is easy to calculate the surface area of an idealized case of cubic particles, but in cases of more complicated particle shapes, the relationship gets more sophisticated. However, using an idealized calculation can always provide the order of magnitude for the surface area of more complicated cases.
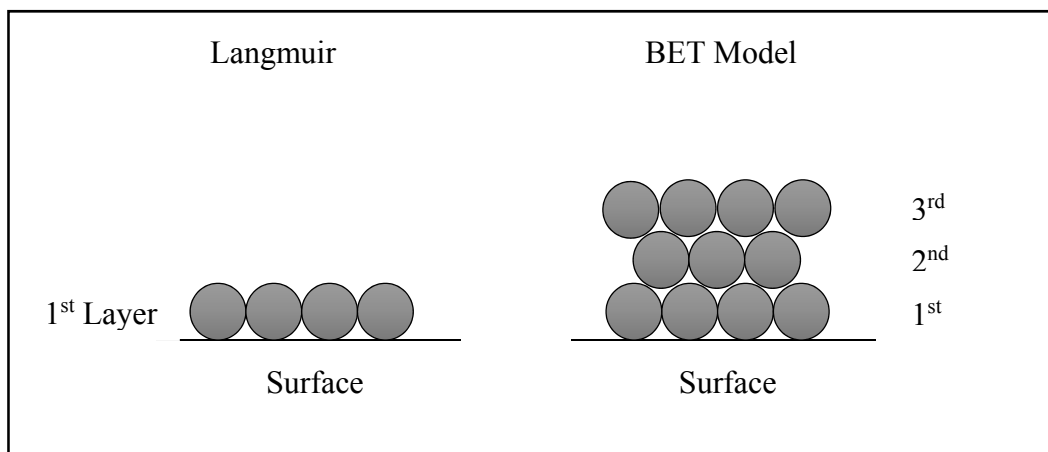
Figure 3 *Comparison of Langmuir and BET adsorption model*

2.2.6 Pore size classification

A given solid does not necessarily have similar pores, and pore systems differ from one solid to another. Pores have so many different characteristics such as width of the pore, diameter of pore in case it is cylindrical, size of pore, etc. Dubinin (32) initially proposed a classification for pores per their width. His classification is now officially endorsed by the International Union of Pure Applied Chemistry, which is shown in Table 2 below (33). The classification is in agreement with the previously mentioned adsorption isotherm trends. It is nearly impossible to draft the isotherm in detail in case of macropore adsorption because pores are wide, and consequently, relative pressures are about unity. In mesopores, capillary condensation occurs. Finally, micropores are holding greater amounts of adsorbate in themselves because adjacency

to walls brings higher interaction between molecules. More than that, the upper limit of the micropore range is not constant and keeps varying form one solid to another.

Table 2 Pore size classification

	Pore Width
Micropores	Less than 2nm
Mesopores	Between 2 and 50 nm
Macropores	More than 50 nm

2.2.7 Isotherm analysis

Isotherm graphs are used to obtain valuable information about surface area and pore size distribution of adsorbent. Type 1 isotherm represents microporous adsorbent. Detailed interpretation of these types of isotherms is still an issue. For example, researchers have not agreed upon the certainty of surface area calculations derived from these isotherms; however, the Type 1 isotherm can still provide an estimation of total pore volume of the adsorbent. This isotherm depicts a monolayer adsorption due to the flat part portion in the graph and can easily be explained through Langmuir adsorption theory. An example of this isotherm would be the adsorption of nitrogen or hydrogen on charcoal at a temperature of about -1800 °C. The Type 2 isotherm is an indication of an undetermined multilayer formation which shows a large deviation from Langmuir model. This behavior is found in adsorbents with wide distribution of pore sizes such as microporous solids or nonporous ones. Moreover, it is possible to acquire the specific surface of solids out of Type 2 isotherms. Type 3 isotherms are less common than other isotherm types and indicate a weak interaction between adsorbate and adsorbent molecules. As there is no flat portion in the Type 3 isotherm graph, this illustrates a non-porous solid with the formation of multilayers of adsorbate on the surface of adsorbent. Relative pressure of adsorbate

in this isotherm type approaches unity. Type 4 isotherms are characteristic of a mesoporous solid and helps evaluate the pore size distribution of the solid. Lower pressure region of this graph is similar to Type 2 isotherms which demonstrate formation of monolayer followed by multilayer. The relative pressure curve in this isotherm finishes near unity. The Type 5 isotherm shows similarity to the Type 4 isotherm as they both represent capillary condensation of gas with a hysteresis loop between the adsorption and desorption branch. Perpendicular branches of adsorption and desorption around the relative pressure of 0.5 confirm the presence of mesopores in the solid. Lastly, Type 6 is a representative of a stepwise multilayer adsorption isotherm (26).

Carbon dioxide is an example of an adsorptive material and has a simple molecular structure. However, its adsorption isotherm is very responsive to the ions and polar groups' presence on the surface of the adsorbent. There is also the possibility of chemisorption in this case which complicates its isotherm analysis.

2.3   Review of measurement's methods

2.3.1   Porosity measurement

Porosity is a measure of void volume or free pore space in a solid, which can be occupied by a specific fluid and is expressed in volume fractions of the substance. It is beneficial to define void and pore as separate terms. A void is a free space in a solid comes to existence, due to discontinuity in array of atoms and molecules. Pore is a type of void, which is connected to the external surface of the solid allowing flow of fluids into, out of, and through the material. Closed pores and open pores terms are also used in scientific world, referring to not so connected voids and connected to the external surface respectively (34). According to Levine, this available

volume fraction in coal, which is supposed to be occupied by fluid, varies from one fluid to another (35). Density, specific gravity, and other physical properties of a substance are dependent on its pore volume percentage. The more pore volume available in substance, the less density it possesses and vice versa (36) .

There are a number of different classifications for coal pores in literature, and most of them confirm the results coming from high-resolution electron microscopy (34, 37)

Coal is in fact characterized as a dual porosity substance including micropore and macropore system, and there are several methods to capture coal porosity and its distribution. Table 3 summarizes the methods of coal porosimetry (35).

Table 3 *Methods of porosity measurement (35)*

Category	Scattering methods	Microscopic methods	Fluid probe methods
	small angle X-ray scattering	optical microscopy	volumetric fluid displacement
Method	electron scattering	Scanning electron microscopy	vapor sorption studies
			heats of wetting
	neutron scattering	transmission electron microscopy	NMR spectroscopy
			ESR spin label probe

Small Angle X-ray Scattering (SAXS) is a reliable method to evaluate total porosity. This method is nondestructive to the sample and gives a fast measurement of porosity without contacting to any chemicals. It takes both open and closed pores in the system into account and may be used to capture pores with diameters from one nanometer to two micrometers, which is

within the range of coal's pore diameter. SAXS assumes there are only two phases in the substance; pores and matrix. Mineral content is ignored (38).

Small Angle Neutron Scattering or SANS is another experimental technique to measure porosity in mesoscopic scale, employing elastic neutron scattering at small angles. This method is quite similar to SAXS, but is known to have some advantages over SAXS, such as the sensitivity to light elements (39).

Scattering techniques take into account the heterogeneity of the samples, and provide information in agreement with the adsorption methods of porosity measurement. SAXS method has been used for over half a century now and has provided promising results. Many works have been done on coal characterization using scattering methods. These techniques demonstrate that during activation of carbon, growth of mesopores occurs concurrently with the reduction of micropores (40).

Nuclear Magnetic Resonance (NMR) spectroscopy method has become the only applicable method of porosity measurement in case of partially filled and dual phased pore systems (41).

In **Volumetric Fluid Displacement Method** for porosity measurement, a certain amount of water is poured into a graduated cylinder. Next, a measured volume of coal is placed into a graduated baker and is compacted. The compacted coal sample is poured into the cylinder and by recording the new cylinder volume, coal porosity can be calculated. The method of volumetric fluid displacement was used to see the relationship between coal porosity and amount of air leakage in underground mining coal seam in China (42).

One of the most successful methods of porosity evaluation is based upon BET surface area measurement of gas adsorption process. As an example of **Sorption Study Porosity**

17

Measurement, porosity of coal with four different gases (N_2, CO_2, He, and CH_4) has been studied and experimented with Langmuir sorption apparatus. Results stated that helium is the most successful gas in case of porosity measurement due to its small molecules' size (43).

2.3.2 Pore size distribution measuring techniques

In a typical porous media, the pore sizes are distributed expansively over various size values generating a pore size distribution system. Pore size distribution is usually presented as a probability density function. There are different methods of obtaining the pore size distribution of a porous solid among which mercury intrusion, porosimetry sorption isotherm and image analysis are the most popular. Mercury intrusion method works better for large pore systems and as for smaller pore networks, sorption isotherm is the best. However, to comprehensively analyze pore size distribution of a porous media, a combination of all three methods would be beneficial.

Mercury Porosimetry

Characterization of a solid's porosity through mercury porosimetry method employs different levels of pressure enforcement onto the immersed material in mercury. Required pressure to let mercury into the material is inversely proportional to the size of the pores, assuming a cylindrical pore shape. Using modified Young-Laplace equation gives the pore size distribution of the material. There are limitations and disadvantages associated with this method such as underestimating the pore sizes. The reason is that mercury does not diffuse into closed and internal pores; it rather measures the large pores starting from 3.5 nanometers.

Sorption Method

Adsorption-desorption measurement method is primarily for surface area calculation and gives porosity, average pore size and pore size distribution based on condensation with capillary pressure increase. Condensation first takes place in small pores and proceeds to larger pores (44). There are numerous models for adsorption of gases into solid materials to analyze surface area and pore size distribution. Density functional theory (DFT) is a popular model based on statistical thermodynamic for obtaining pore size distribution. Molecular modeling and numerical simulation, such as Monte Carlo, are other examples of statistical techniques (45). Institute of coal chemistry in China carried out extensive study on adsorption of various carbonaceous materials such as coal activated carbon, pitch carbon beads and employed density functional theory to obtain pore size distribution. They concluded that DFT method could present pore size distribution in a wide range from micropores to macropores with just a single analysis (46).

Micro Tomography

Micro tomography is a newer tool to capture pore size distribution of porous materials with X-Ray. The apparatus holds about 1 cm of the sample and exposes the sample to X-ray beams so that a 3-D picture of the sample is generated. This method can also provide mineral content in materials and total porosity (44).

2.3.3   Adsorption measurement methods

Several researchers have developed techniques for measuring adsorption amount of fluid on adsorbents. Gravimetric method, volumetric method, chromatographic method, piezometric method and IR spectroscopy are among conventional methods of measurement. There are also newer techniques for adsorption calculation such as frequency response technique (FRT), total

desorption and zero column methods. Methods and techniques are discussed briefly in the following (47).

Gravimetric Process is based on recording weight change of a sample as the partial pressure of the adsorbate varies with the use of a sensitive balance. This method gives a continuous measurement of the adsorption amount at each equilibrium pressure point at a fixed temperature. This method can also be used to determine density of the samples using an inert gas. Gravimetric sorption analyzer has two separate methods of process, one for static systems, in which a fixed pressure of a single gas is let into the system, and dynamic systems, which supports flowing gas environment (48). This method only accommodates pure gas investigation and experiments cannot be repeated.

Volumetric Method is basically expanding the volume of a gas in a known-volume cell, referred to as reference cell, into an already evacuated cell known as sample cell, which includes the adsorbent. The whole system is kept isothermal during the experiment and using transient molar balance of components, adsorption amount is obtained. This method has been frequently used in studies because of its simplicity. However, there is no control over final data points and once the adsorbate is let into adsorbent cell, it is difficult to repeat the experiments as the gas in already adsorbed onto the sample at the certain condition.

Piezometric Method. In this method, weighed adsorbent is placed into a glass ampule and then located in thermostated vessels of bulbs linked with capillary tubes. Pure gas is allowed to the vessel and ampule is broken to let adsorbent get in touch with the gas. Pressure and density of equilibrium gas is recorded and used to calculate pure gas GSE isotherm. This method is ideal for high-pressure data acquisition.

Combination Gravimetric-Volumetric Method is used for measuring isotherm of a binary gas mixture. This approach does not require final gas equilibrium analysis as needed in volumetric method. There is no control over final data points and kinetic measurements are not suitable for this method.

Total Desorption Method. In this method, adsorbent is put into a column with a known void volume and is saturated with gas mixture in an isothermal condition. By heating and evacuating the system, adsorbed components desorb from the column. Desorbed volume amount is measured, along with density and pressure of the collected gas, and substituted into the GSE equations for adsorption calculation. This method does not apply to kinetics of adsorption but is easy to repeat, and the final state of the data points is under control.

Column Dynamic Method. This method supports both adsorption and desorption experiments and is good to capture trace adsorbent in bulk gas. The experiments are conducted at a fixed pressure and temperature and require precise flow rate and composition measurement.

Closed Loop Recycle Method. As one of the advantages of this method, it can be pointed out that this method is suitable for measuring multicomponent adsorption of trace in bulk. There is a chamber that holds the adsorbent and is placed in a closed loop system with an inline gas recycling pump. The entire system is kept isothermal and the measurement process starts by circulating gas through the sample chamber and recording the transient and equilibrium concentration of the traces. This method is again difficult to repeat and there is no control over final results.

Isotope Exchange Method. This method is known as an especial case in closed loop recycle adsorption method discussed earlier. The interesting feature of this method is that adsorbed gas

phase remains isothermal along the process, while in all other methods, due to consumption of heat, adsorption kinetic systems becomes non-isothermal and makes the analysis complicated. Another advantage of this method is the control over final pressure of the system, which was undoable and random in other methods (47).

2.4 Gas adsorption on coal

Amount of gas adsorption on coal is a highly dependent parameter. Coal seam properties and composition, temperature at which adsorption occurs, pressure of the formation and adsorbate, moisture content of the coal and adsorption gas type are some of the effecting parameters in adsorption process. Hence, it is beneficial to further study all affecting parameters in order to have a better understanding of the whole gas adsorption concept on coal.

2.4.1 Effect of physical properties of coal

Many researchers have reported the effect of coal minerals and maceral, ash content, moisture content and carbon content on gas adsorption capacity of coal (49).

Figure 5 shows findings about the physical properties' effect of coal on adsorption capacity. Coal is described to contain three main macerals named liptinite, vitrinite, and inertinite, among which Vitrinite is positively impacting the adsorption capacity of coal. The reason is stated to be the presence of micropores in vitrinite. On the other hand, liptinite is reported to hold macropores, therefore, the more liptinite available in coal, the less room is left for highly porous vitrinite maceral which validates the reduced adsorption capacity (50-55). Regarding inertinite content effect on adsorption capacity, no direct relationship is proved yet (56).
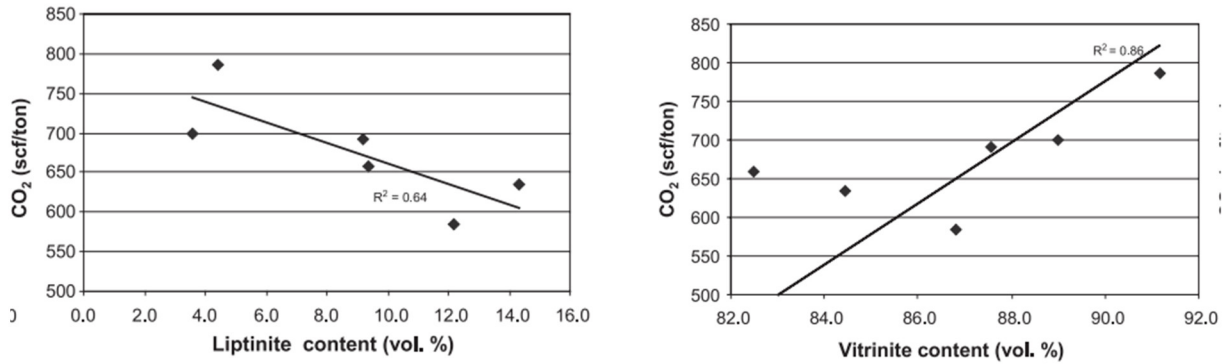
Figure 4 Effect of Vitrinite and Liptinite content on adsorption value of CO_2 (57)

As per mineral matter content in coal, reports show that minerals in coal negatively influence the capacity for adsorption. The reason is mentioned to be low capability of mineral to adsorb gas on their surface. Consequently, the presence of limited adsorption capacity parts in coal reduce the ready to use space for maceral in coal (58-60).
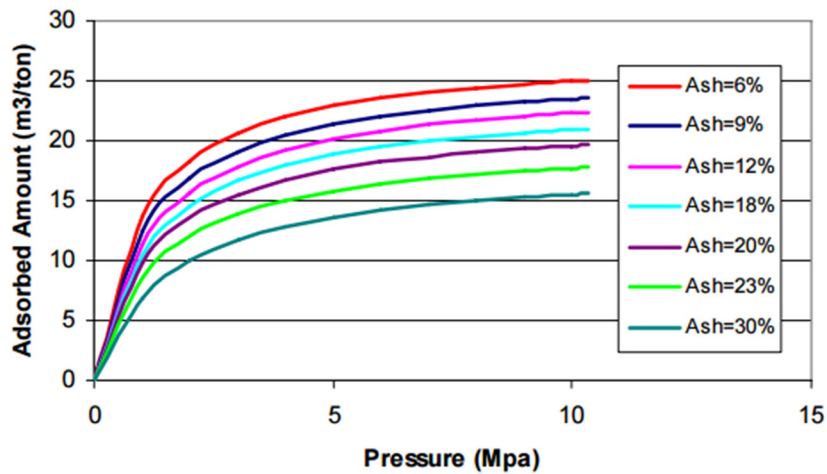
Figure 5 Effect of Ash content on adsorption isotherm (57)

Gas molecules tend to adsorb on the organic surface on coal, even if an inorganic surface is also available. Thereupon, ash and mineral matter presence as an inorganic part in coal causes reduction in coal capability of accommodating gas in itself (61-65). Different carbon content in

23

coals is caused by different exposure of coals to burial pressure and heat, as well as the amount of time for formation. The relationship between the carbon content of coal and adsorption capacity is not linear and is observed to be a U-shaped curve. At the bottom of this curve, medium volatile bituminous coal is placed. In other words, adsorption capacity of coal decreases with an increase in carbon content until it reaches the amount of 83.5% of fixed carbon and continues to increase afterward (52, 56, 66, 67).

The next consideration affecting parameters on adsorption is the moisture content of coal. Moisture in coal surfaces creates a film, which limits the adsorbate's contact with the coal surface and results in adsorption reduction. Moisture content has a critical saturation meaning that after a certain amount of moisture content in coal, moisture starts to mobilize and stops any further reduction in adsorption (55, 61, 68).

2.4.2 Effect of gas type on adsorption
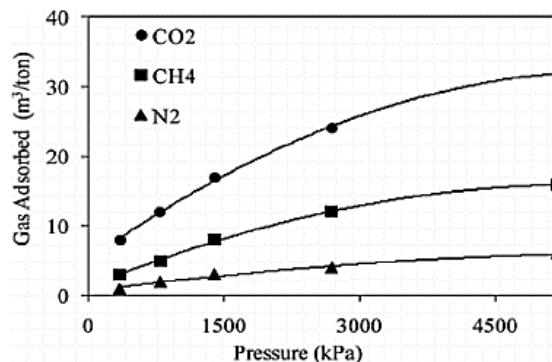
Figure 6 *Variation of gas adsorption capacity of coal for different types of gases (62)*

The type of adsorption gas has definitely an important effect on the amount of adsorption in solids. Among typical gases as adsorbate such as carbon dioxide, nitrogen, and methane, carbon dioxide is reported to have higher adsorption capacity due to strong intermolecular forces

between CO_2 and coal molecules. This forceful bond causes methane to be replaced with carbon dioxide in enhanced coal bed methane recovery process.

According to the findings about gas type effect on adsorption, nitrogen has the least adsorption capacity followed by methane and carbon dioxide (12, 58, 69).

2.4.3 Effect of temperature on adsorption

The process of adsorption is an exothermic reaction. Therefore, it is expected that with a rise in temperature, adsorption capacity decreases. In the case of physisorption, the results confirm that the adsorption amount decreases as temperature increases because Vander Waals forces are strong at low temperatures.
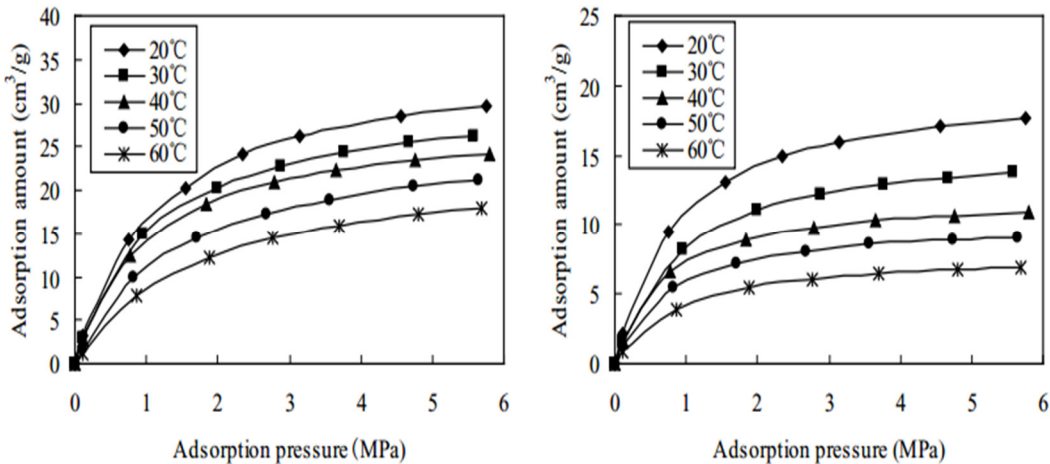
Figure 7 Effect of temperature on adsorption isotherm (71)

However, in the case of chemisorption, adsorption capacity increases with temperature rise, which is an indication of activation energy requirement for chemical reaction, and continues to decrease after reaching a peak (63, 70, 71).

2.4.4   Coal swelling and deformation during CO_2 adsorption

Carbon dioxide is reported as the most adsorbable gas on coal among other field-tested gases such as methane and nitrogen (72). However, the adsorption of CO_2 on coal induces coal swelling, which leads to permeability reduction. Coal swelling and the deformations of pores followed by it, is dependent to the carbon content in coal (73, 74). The permeability of powdered coal samples was measured in Korea and was plotted versus pore pressure (adsorption pressure). The results indicated that the permeability of the samples decreased as the pore pressure increased (75). It is reported that the pores smaller than 0.5 nm expand as the pressure increases; on the other hand, pores larger than 0.5 nm shrink as the pressure goes up to 10 MPa and expand thereafter (76).

2.5   Adsorption capacity of pyrolyzed coal

The initial step of coal utilization in combustion, gasification, and liquefaction is pyrolysis at high temperatures. The organic structure of coal decomposes once exposed to a high heating rate and releases its volatile matter. Tar as a separable and condensable component of coal solid at room temperature is also formed during coal pyrolysis (77). Volatile matter and tar may be up to 70% of coal mass and lead to the formation of semi-char (78, 79).

The findings show that in coal pyrolysis with temperatures up to 800 °C, the total porosity of coal increases due to an increase in micropores and mesopores. Generation of newly formed pores due to volatile matter removal as well as opening of closed pores are the primary mechanism of pore structure at temperatures below 650 °C. Additional changes and enlargements are a result of structural rearrangement (79, 80).

There have been numerous studies on CO_2 adsorption on coal chars, a number of which are discussed below. Samples of lignite, sub-bituminous, and bituminous virgin coals and their char have been de-volatized in nitrogen at 1000 °C to 1300 °C. This experiment was performed at West Virginia University and the carbon dioxide adsorption capacities on samples were reported. All pyrolyzed samples in this study showed higher adsorption values in comparison with the virgin coal (81). Other research has been done in Cairo to obtain the adsorption isotherm and surface area of a sub-bituminous coking coal and its carbonization products with methanol, benzene, nitrogen, and cyclohexanone. Similar results were observed and showed that carbonization products have higher adsorption capacities in comparison to virgin coal samples; the value of the adsorption also rises up to a certain temperature that varies from gas to gas (82). Experiments on Japanese non-caking and caking coal, which have been exposed to 100 °C to 900 °C with carbon dioxide as the agent gas for adsorption, exhibits an increase in the pore volume up to about 700 °C. Adsorption capacity then decreases due to pore structure shrinkage (83). The same results were observed in Ontario, University of Waterloo, based on carbonization temperature of 400 °C to 1000 °C, and a maxima of porosity, pore volume, and surface area were noticed at temperatures about 700 °C (84).

There are also studies about pore structure change after coal gasification with different conversion levels. Pore structure development at different temperature and conversion level of gasification in air and carbon dioxide was studied by Argon adsorption at 87 K in Australia. Results of their works show that in gasification with air, surface area and pore volume of small pores do not change as opposed to larger pores. The change in small pores surface area and pore volume displays an increase with carbon conversion increase during the gasification process (85). The conversion rate of coal gasification in the mixture of CO_2 and H2O at high pressures

is used to demonstrate the mixture effect (86). In addition, kinetics of coal gasification and its reactivity along with its dependency on pressure, heating rate, and particle size is proposed in Washington University (87). Finally, adsorption behavior of virgin coal and pyrolyzed coal char, which have been exposed to 800 to 1000 heat in furnace with CO_2 up to 65 bar, were investigated. The influence of coal properties such as vitrinite content, coal rank, volatile matter, ash content, and surface area were reported. It was mentioned that the adsorption capacity increases when changing from virgin coal to pyrolyzed coal (10).

Chapter 3

3 Experimental Method

3.1 Sample preparation

There were two stages of sample preparation in this study. The first stage belongs to underground coal gasification process experiments in which a cylindrical coal core is arranged to go under high temperate and gasification processes and thus produces syngas and pyrolyzed/gasified coal chars. The second stage is to take out small samples from different areas of this coal after the gasification process is done. Further explanation for detailed preparation is discussed below.

3.1.1 Preparation of coal block

Coal samples for gasification process are supplied by Shertitt International. A mixture of coal for the block was made using 8:1:1 ratio of one-centimeter coal particles to coal powder to cement by weight. Water was added to this mixture to obtain a uniform consistency. This mixture is then poured into a cylindrical tube shape made of concrete, which holds the mixture inside it and resists heat loss. The block is then allowed to dry for several days to solidify. Several 5 mm diameter holes were drilled into the block to accommodate injection and production wells, a spark igniter, and a few thermocouples to monitor the block temperature during the gasification process. A link between the production and the injection wells are required for this gasification method, hence, an empty channel of 5 mm diameter is drilled along

the length of the coal block at two third of the core diameter from the top (top is the position on the tube along which the holes are drilled).

Figure 8 Sample preparation for UCG experiment

The coal block is next sealed with flanges and gaskets using nuts and bolts and is placed into the UCG apparatus for gasification. Successful fire for igniting the coal for gasification startup happened at pressure of 5 Psia, temperature of 22 °C, and 20 % of excess oxygen, with a propane concentration of 14.3%. Initial oxygen flow rate was 2 L/min and once the block temperature reached the temperature in which self-burning occurs (investigated to be at around 450 °C), propane supply is stopped.

Upon completion of the experiment, the concrete tube was taken out of the vessel and sent to the Earth Science building at University of Alberta to be cut for the volumetric adsorption measurement experiments' sampling. The core was first cut down in the middle and two 10-inch cylinders of coal were made. Then a section of the outer tubes from each half was cut lengthwise from the top in order to give access for sampling, and the half closer to the ignition

channel was sampled for volumetric adsorption setup. Figure 13 shows the sampling process step by step.

Figure 9 Sample preparation for volumetric adsorption measurement setup
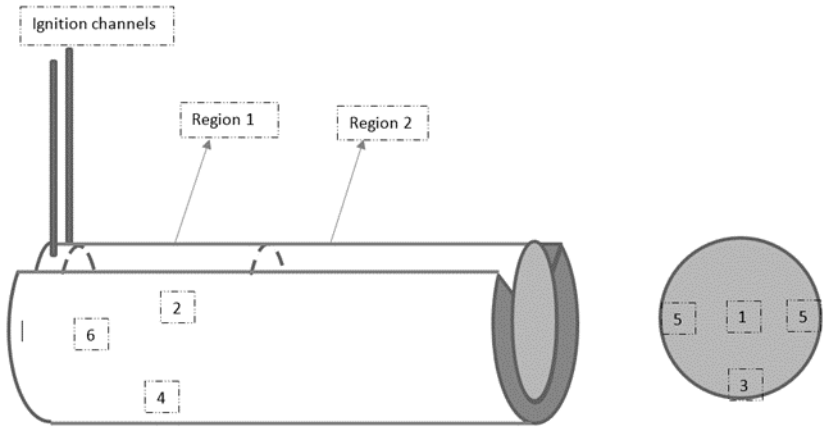
Figure 10 Sample position map

Figure 10 shows the sampling map for adsorption measurement experiments.

According to the sample map, six samples were taken from two regions of the core. The positioning is also further explained in Table 4.

<p align="center">***Table 4*** *Coal sample positioning details*</p>

Sample Number	Region number	Description
1	Two	Middle of the core
2	One	Middle of the core
3	Two	Bottom layer
4	One	Bottom layer
5	Two	lateral layer
6	One	lateral layer

During the cutting process, water was coming from the instrument to cool down the blades. Hence, samples were taken to the oven with a temperature of 105 °C and were left there for 24 hours for moisture removal.

3.2   Volumetric adsorption setup preparation

In consideration of measuring adsorption capacity of gasified coal samples, a volumetric apparatus with relatively large sample cell (41cc) was designed to better capture heterogeneity of the samples. This apparatus was already used to measure adsorption capacity of pyrolyzed coal samples in 2014. Only minor changes were applied to the setup, like changing the size of tubing for its new location in the lab and installing new relief valve to ensure safety. Figure below shows the schematic of the updated volumetric adsorption apparatus.

There are four main sections in the volumetric setup for adsorption. Gas injection, an isothermal section, an evacuation section, and a data acquisition part. the gas injection segment consists of a high-pressure syringe pump (ISCO 500 D) with a delivery of maximum 3750 psig, and a pressure relief valve on the way from the pump to the system set for 2500 psig to ensure safety. A reference cell, a sample cell, a pressure transducer (to monitor reference cell pressure and system pressure), temperature thermocouples, valves and plastic spheres are all placed in the isothermal section of the setup which is equipped with a high accuracy temperature controller
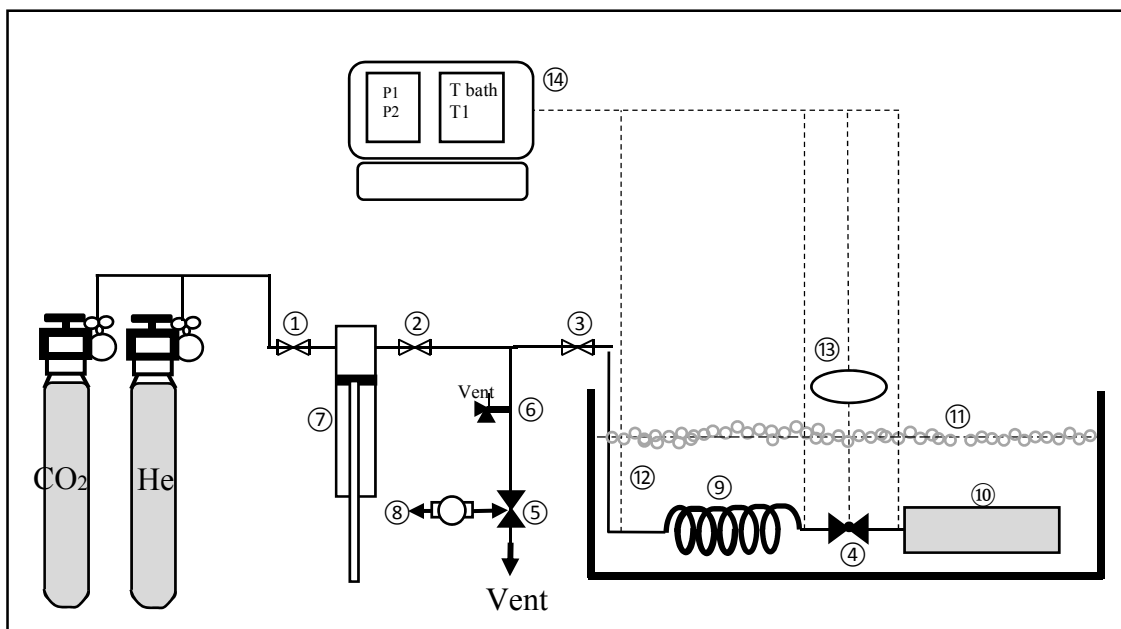
Figure 11 *schematic of the volumetric adsorption apparatus [1-5 valves, 6: pressure relief valve, 7: high-pressure syringe pump, 8: vacuum pump, 9: Reference cell, 10: sample cell, 11: solid sphere for isothermal isolation, 12: water bath, 13: pressure transducer, 14: data acquisition system*

(Thermo Scientific model 253). Temperature was kept constant by both setting the water bath temperature for 45.5 °C and laying plastic spheres on the water bath surface to avoid any heat exchange with the atmosphere. Two different temperatures are constantly recorded; water bath temperature and T1. T1 is placed between the reference cell and the sample cell and reports gas temperature in cells. Temperature is one of the critical factors controlling the amount of

adsorption of gases; therefore, it should be kept constant and monitored continuously. The reference cell and the sample cell are accommodated with inline filter to stop solid particles from entering the tubing and plug them. An O-ring was used in the sample cell to seal and ensure no gas leakage is found. The Sample cell itself has a tiny hole, which sends out bubbles if there is any leakage in the system. The evacuation section includes a vacuum pump, which helps remove any tracing gas in the system, and a valve that allows gas to be vented to the fume hood. Finally, the data acquisition segment records pressure and temperature values every 10 seconds in an excel file with the help of the TRH central lab and lab view program. Specifications of the volumetric apparatus are listed in the Table 5.

Table 5 *Volumetric adsorption setup specifications*

Parameter	Value
Reference cell volume	31.25374
Sample cell volume	41.14325
Volume ratio	1.3164
Pressure transducer accuracy	0.0025% of the span
Pressure transducer span	400-3000 Psia
Temperature accuracy	$\pm1°C$
Pressure and Temperature recording step	10 seconds
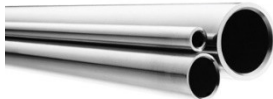
The procedure of measuring the adsorption capacity of samples is briefly as follows. The Sample is placed in the sample cell, and gas is injected into the reference cell and remains there until it reaches equilibrium. After about two hours, the valve between the reference cell and the sample cell opens and gas starts to adsorb onto the coal sample. This stage requires a longer

34

time to reach equilibrium, which is approximately 22 hours. In this research, Gibbs excess adsorption equations were used to calculate the amount of adsorbed gas on the sample. Equations for adsorption measurement have several unknown values, which could be measured prior to the start of the experiment and while the experiment is running. Unknowns are the reference cell volume, the sample cell volume, and the void volume in the system (the existing volume for gas to occupy) plus temperature and pressure of the gas. Details are explained in the operating procedure section.

3.3 Volume calibration method

Volume calibration of the reference cell and the sample cell was performed with both physical measurement and constant volume gas pycnometery method of the helium blank test. In both methods, the volume of the associated valves, connections, and connected parts of the tubing to the cells were also included. In the physical method, the volume of each component was calculated from the dimensions specified in Swagelok catalog or by physically measuring the dimensions. For example, in order to determine the volume of the tubing, the outer diameter of the tubing, the wall thickness and the length of the tubing are needed to incorporate cylinder volume calculation formulas. Table 6 summarizes the specifications of one of the tubing used in the volumetric setup.

Table 6 *Volumetric adsorption setup Tubing specifications*

Part name	316/316L Stainless Steel Seamless Tubing, 1/4 in. OD x 0.065 in. Wall x 20 Feet
Part ID in Swagelok	SS-T4-S-065-20
Material	Stainless steel
Tube OD	¼ in.
Tube wall thickness	0.065 in.

In the pycnometery method, a stainless-steel sample cylinder is used as the known volume of the pycnometer, which will be called "added volume cell" from now on. Both the reference cell and the sample cell of the adsorption setup should be calibrated. Therefore, the pycnometery method calculations are repeated two times: once to obtain the reference cell volume, and secondly to determine the sample cell volume. In order to measure the volume of the reference cell, the pycnometer cell is connected to the reference cell and the valve between two cells is closed. Helium is then injected to the added volume cell, and the reason helium is chosen is because helium is the cheapest inert gas, which has the smallest molecule size. The Pressure of the added volume cell is recorded and the valve between cells opens to allow helium to travel to the reference cell to equilibrate. With the value of the final pressure and Boyle's law, the

volume of the reference cell is determined. This process is then repeated with the calibrated

reference cell assigned as the added volume cell and the sample cell as the cell to be calibrated.
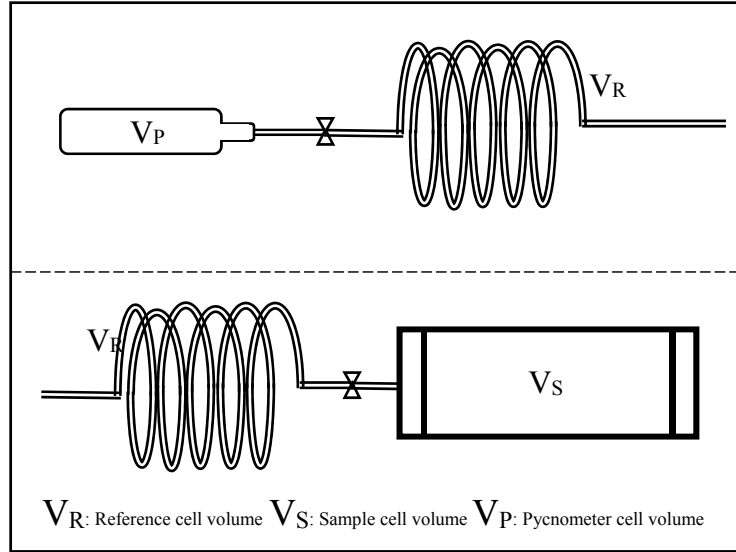
Figure 12 Volume calibration method clarification

Reference cell volume calibration:

$$P_1 V_1 = P_2 V_2 \quad Boyle's\ Law \quad (3.1)$$

$$V_R = \frac{(P_1 - P_2)V_P}{P_2} \qquad (3.2)$$

P_1: pressure of added volume cell

P_2: pressure of cells after t e valve opens

Sample cell volume calibration:

$$V_S = \frac{(P_1 - P_2)V_R}{P_2} \qquad (3.3)$$

P_1: pressure of reference cell

P_2: pressure of cells after t e valve opens

The final calibrated volumes were chosen in such a way that least error was observed.

3.4   Gibbs surface excess energy measurement

Two different gas phases exist during the gas adsorption process, which are separated through an interface. The Adsorbed gas phase is referred to as the gas present on the adsorbent surface and the bulk gas phase is any gas which is in the system but is not adsorbed on the surface of the adsorbent. These two phases have different physical properties, such as density, which are difficult to measure.

Excess Adsorption or Gibbs Surface Excess (GSE) Adsorption is defined as the difference between the amount of gas adsorbed at the bulk gas phase density and the amount adsorbed at the adsorbed gas phase density. In this research, with the help of Gibbs surface excess adsorption equations, which will be illustrated below, the amount of adsorption on coal surface is measured and reported.

3.4.1   Single pressure mode

In order to calculate the amount of gas adsorbed on the coal surface, mass balance equations need to be written. Initially, gas is injected into the reference cell, and the amount of gas in a volumetric adsorption system is equal to the volume of the reference cell (V_R) (inclusive of all fittings and valves) times by the molar density (ρ_1) of the gas inside the cell.

$$n_{initial} = \rho_1 \times V_R \quad (3.\ 4)$$

After the valve between the reference cell and the sample cell opens, and equilibrium takes place, the mass balance equitation in the system can be written as:

$$\rho_1 \times V_R = \rho_2 \times V_R + \rho_2 \times (V_{cell} - V_{solid} - V_a) + \rho_a \times V_a \quad (3.5)$$

V_{solid} is the volume of just the coal and does not include the pore volume inside the coal sample.

V_a and ρ_a are the adsorbed gas phase volume and density.

From the definition in Gibbs excess adsorption model, excess adsorption value is:

$$n_{excess} = V_a(\rho_2 - \rho_a) \quad (3.6)$$

If n_{excess} is substituted in the original mass balance equation, the final excess adsorption equation will be as follows:

$$n_{excess} = V_R(\rho_1 - \rho_2) - \rho_2(V_{cell} - V_{solid}) \quad (3.7)$$

Helium is used to measure the void volume in the system. Thus, the void volume equation can be written as follows, considering the fact that no adsorption occurs when helium is injected.

$$0 = V_R(\rho_1 - \rho_2) - \rho_2(V_{cell} - V_{solid}) \quad (3.8)$$

The total free space available in the sample cell after helium is injected is known as the Void Volume:

$$V_{Void} = V_{cell} - V_{Solid} \quad (3.9)$$

Therefore, Void volume in the system can be written as:

$$V_{Void} = \frac{V_R(\rho_1 - \rho_2)}{\rho_2} \quad (3.10)$$

Taking void volume into the excess adsorption equation, the final equation can be rearranged like below:

$$n_{excess} = V_R(\rho_1 - \rho_2) - \rho_2 \times V_{Void} \quad (3.11)$$

According to this equation, in order to measure the amount of gas adsorbed on the surface of the coal samples, four unknown values exist: the reference cell volume, the void volume, the reference cell's gas density, and the system density after equilibrium.

3.4.2 Cumulative pressure mode

The Adsorption process cannot be stopped until the final desired pressure point is observed. The reason is because of the adsorption sensitivity to temperature, pressure, and time. Therefore, a cumulative pressure injection is required to finish one adsorption process of multi pressure points. There is a slight change in calculations, which will be illustrated below.

Initial mole of the gas in the system is the same as before:

$$n_{initial} = \rho_1^i \times V_R \quad (3.\ 12)$$

In which ρ_1^i is the density of the injected gas to the reference cell at that current step. Consequently, the mass balance equation for the ith step becomes:

$$\rho_1^i \times V_R = \rho_2^i \times V_R + \rho_2^i \times (V_{cell} \quad V_{solid} \quad V_a^i) + \rho_a^i \times V_a^i + \rho_1^{i-1} \times$$
$$(V_{cell} \quad V_{solid}) + n_{excess}^{i-1} \quad\quad (3.\ 13)$$

ρ_2^i and ρ_2^{i-1} refer to gas density after the equilibrium at the ith and $i \quad 1^{th}$ pressure points and V_a^i and ρ_a^i are volume and density of the adsorbed gas phase at the current point. Finally, n_{excess}^{i-1} is the excess adsorption of the $i \quad 1^{th}$ point.

To simplify the above equation, another systematic method for calculation is represented.

1. Calculate the adsorbed volume of the current stage
2. Update void volume of the cell
3. Calculate the excess adsorption of the current stage with the updated void volume

4. Add the amount of the excess adsorption of the previous stage to the current excess adsorption value to get the ultimate excess adsorption of the stage

If i=1:

$$V_a{}^i = n_{excess}{}^i / \rho_a{}^i \qquad (3.\ 14)$$

$$V_{void}{}^i = V_{void}{}^{initial} \quad V_a{}^i \qquad (3.\ 15)$$

If i≠1

$$V_a{}^i = V_a{}^{i-1} + n_{excess}{}^i / \rho_a{}^i \qquad (3.\ 16)$$

$$V_{void}{}^i = V_{void}{}^{i-1} \quad V_a{}^i \qquad (3.\ 17)$$

And finally

$$n_{excess}{}^{ultimate} = n_{excess}{}^{i-1} + n_{excess}{}^i \qquad (3.\ 18)$$

3.5   Operating procedure

There are several volumetric methods to calculate the amount of adsorbed gas on coal samples. However, in this research, the single pressure method with cumulative adsorption was used. Running experiments have two main stages. The first stage of the experiment is to measure the void volume in the system (the existing volume for gas to occupy). Helium is used for void volume measurement because helium is an inert gas. Additionally, due to the small size of the helium molecules, it is expected that they go into all pore sizes. Moreover, no adsorption happens on coal with injecting helium into the system. The second stage is to vent and vacuum helium and to inject carbon dioxide to adsorb on coal. Prior to the starting of the experiment, a vacuum of 3 Psia was run to evacuate any trace gas in the system. Helium is then injected into the reference cell and pressure is monitored and recorded for one hour. After an hour, the valve

between the sample cell and the reference cell opens to allow helium to go inside the pores of the sample, which again takes one hour to reach equilibrium. Recorded reference cell and sample cell pressure gives the void volume in the system using the equations in the previous part. The void volume measuring experiments were repeated three times for each sample to ensure the accuracy, and an average of these void volumes was used for the adsorption calculations. Therefore, helium is then evacuated with the vacuum pump and vented out every time.

Figure 13 shows the helium injection along with the single pressure mode procedure for adsorption measurement. Helium injection is repeated three times in real experiments to ensure accuracy.
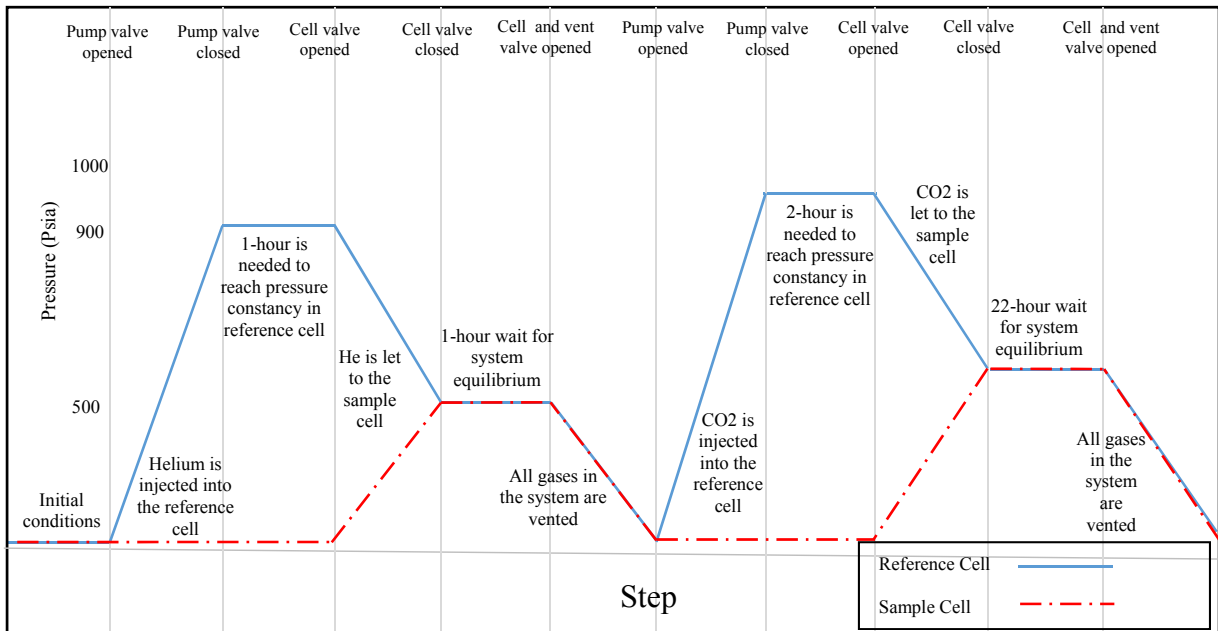
Figure 13 *Procedure for gas adsorption measurement in a single pressure mode*

The next stage is to inject CO_2 for adsorption but before that, all tubing lines and pump are evacuated to make sure no helium is left in the line. CO_2 is injected to the reference cell. Trial and error proved that two hours is needed to reach equilibrium in the reference cell, which is filled with carbon dioxide. Then the valve between the reference cell and the sample cell opens and CO_2 from the reference cell is allowed to equilibrate with the sample cell for 22 hours. The reference cell and system pressure is recorded every ten seconds in the excel file. This is the end of the adsorption measurement at initial pressure. In this research, each sample has four to five pressure points from 500 Psia up to 1000 Psia. 1000 Psia is set as the maximum pressure because the critical pressure of CO_2 is 1079 Psia and it is meant to keep the measuring pressure
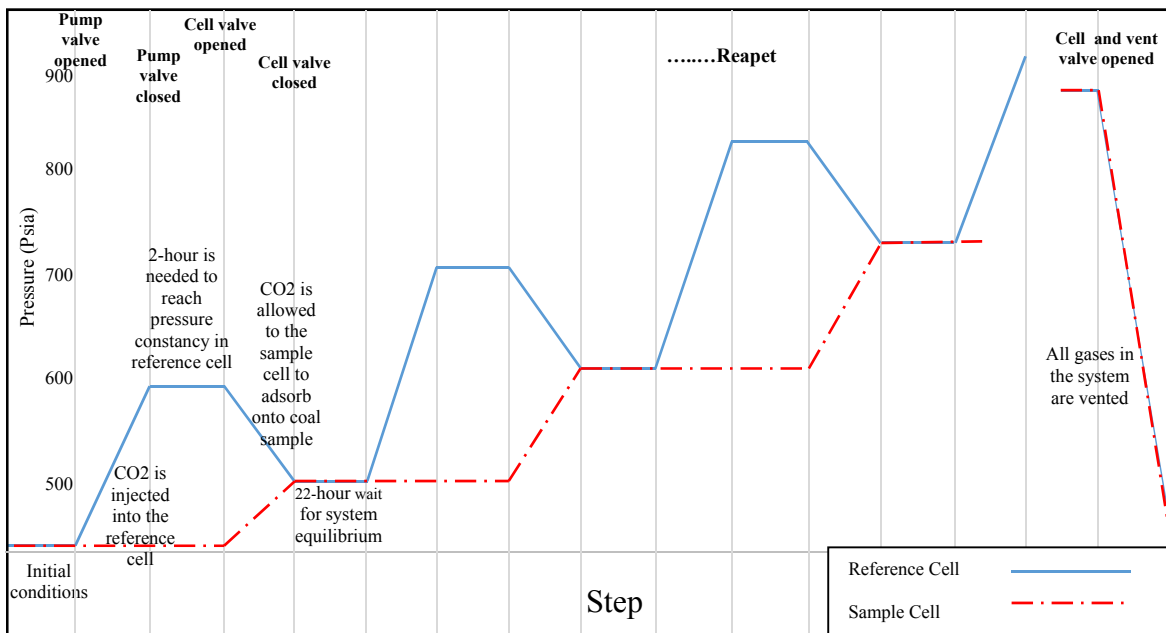
Figure 14 Procedure for gas adsorption measurement in cumulative pressure mode

of the experiments under the critical pressure of CO_2. However, two separate tests were taken for above critical pressures to investigate the adsorption behavior of CO_2 on coal at super-critical pressure. Once the first pressure point is recorded, the valve between the sample cell and the reference cell closes and more CO_2 is injected to the reference cell. A two-hour wait for equilibrium is needed and the valve opens to let CO_2 adsorb onto the sample. The sample is

43

then kept in a sealed container for further analysis. The process is called cumulative adsorption because CO_2 is not vented every time and it is just being adsorbed at a higher pressure-point. Figure 14 shows the procedure for cumulative adsorption measurement. Void volume calculations with helium has been done prior to these experiments and are not shown as steps in the graph.

Figure 15 represents graphs of pressure (Psia) versus time (Second) for two of the helium injections into the reference cell and then to the sample cell on one of the samples.
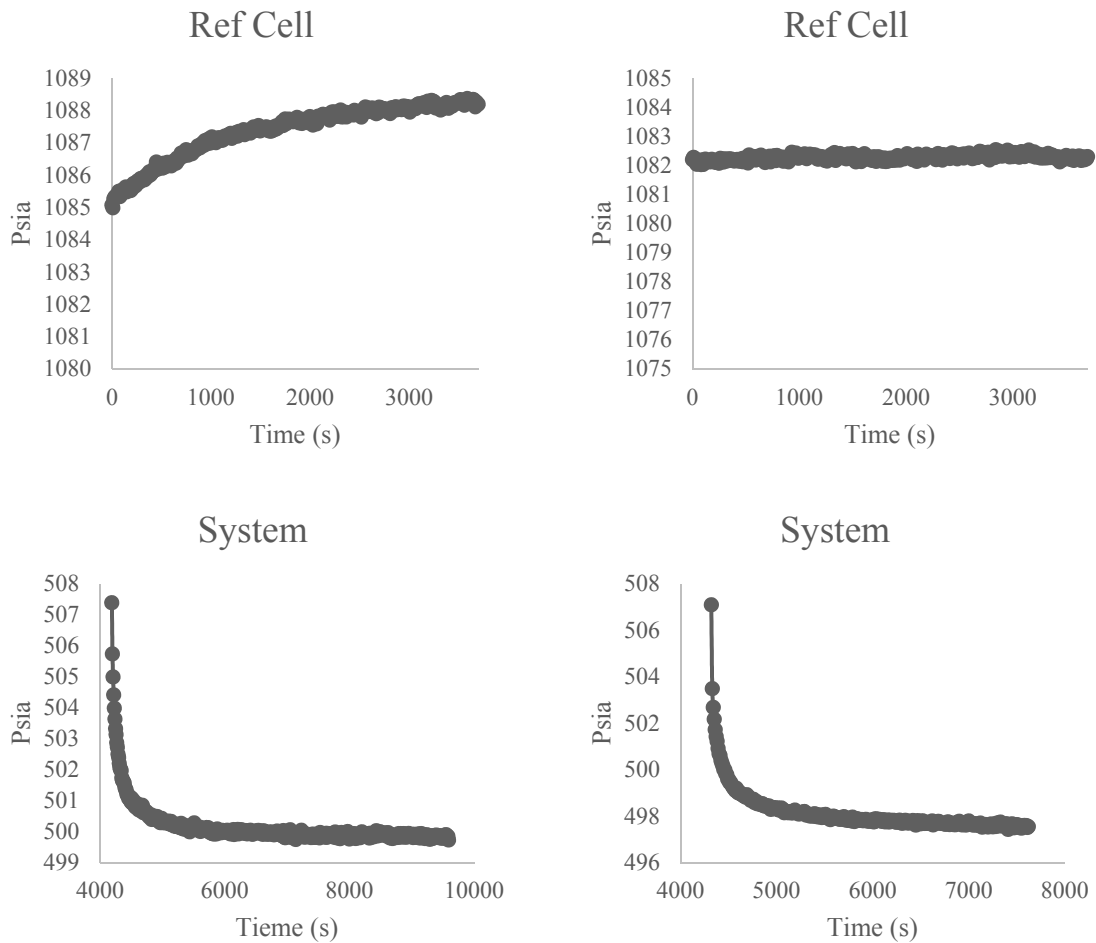
Figure 15 *Helium injection graphs for void volume calculation*

For the reference cell, pressure values from 3550 seconds to 3650 seconds were averaged and used in calculations. Similarly, for the system pressure, values from 7150 seconds to 7250 seconds are averaged and used in calculations. The compressibility factor of carbon dioxide is required to calculate the molar density of the samples. In this study, the Span and Wagner (88) equation is used to calculate the Z factor of CO_2. The equation covers temperatures up to 1100 K and pressures up to 800 MPa. Figure 16 shows compressibility factors from the Span and Wagner equation.
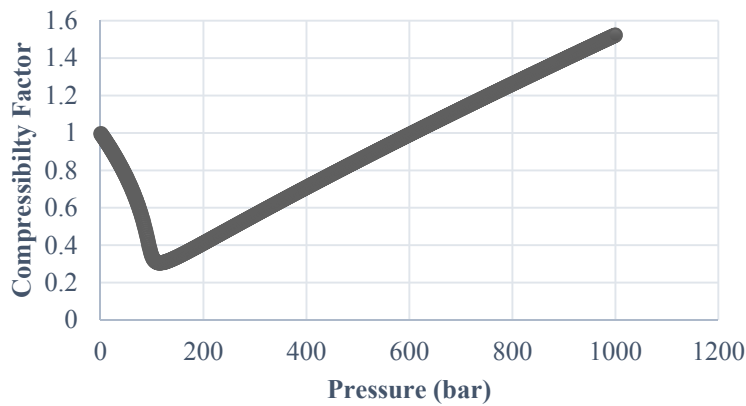
Figure 16 Compressibility factor of carbon dioxide vs pressure at 45 °C

A sample calculation of the void volume and the excess adsorption amount is illustrated in Table 7 and Table 8.

Table 7 Sample calculation for void volume using Gibbs excess adsorption method

Sample Void Volume Calculation		
P1 (Psia)	1088.26	1082.19
P2 (Psia)	499.83	497.57
P1 (bar)	75.0328	74.6144
P2 (bar)	34.4617	34.3059
ρ_1 (mole/cc)	2.6651	2.6499
ρ_2 (mole/cc)	1.2657	1.2598

Ref CEll Volume(CC)	31.25	
Void Volume (cc)	34.55600117	34.48627232

$$\rho_1 = \frac{P1}{zTR} \qquad (3.\ 19)$$

$$Vvoid = V_R \ \frac{\rho_1 - \rho_2}{\rho_2} \qquad (3.\ 20)$$

Using this void volume amount, excess adsorption can be easily calculated as follows:

Table 8 Sample calculation for excess adsorption

Sample 6 Adsorption Calculation			
Ref Cell Vol(cc)	Sample mass(gr)	Void Vol (cc)	Temperature °C
31.25	8.6	31.76	45.25
P1 (bar)		78.14	
P2 (bar)		71.16	
ρ_1 (mole/cc)		5.19	
ρ_2 (mole/cc)		4.26	
Z_1		0.568	
Z_2		0.631	
C_1		266.75	
C_2		266.68	
n excess (mmole)		21.97	
Excess adsorption (mmole/gr)		2.55	

$Z = compressibility\ factor\ of\ carbon\ dioxide$

$C_1 = V_R \ \ \rho_1$

$C_2 = \rho_2 \ \ (V_R + Vvoid)$

$$n_{excess} = C_1 \quad C_2$$

$$excess\ adsorption = \frac{n_{excess}}{sample\ mass}$$

3.6   Coal characterization

Gasified coal samples were taken from different parts of the gasified core in order to capture all sides of the tear-drop shaped residue after gasification. The proximate analysis of the coal samples is reported using the TGA instrument model 701. Nitrogen, air, and oxygen cylinders are connected to the instrument by stainless steel lines to provide the required gases for the thermogravimetric analysis. About one gram of samples are loaded in crucibles and placed inside the apparatus tray to be weighed. The ASTM method is chosen for analysis. All samples have duplicates to ensure that the heterogeneity of samples is considered in results. The first analysis is moisture content measurement. The sample temperature rises to maximum of 110 °C and lasts 30 minutes to ensure all moisture in the sample are gone. Once it is done, the furnace opens and asks for crucibles' lids to be put on and equilibrates the temperature after raising it to 950 °C to start the volatile matter analysis. A carrier gas is needed to take out the moisture and volatile coming out from the samples and for these two stages, nitrogen as an inert gas is used. So far, moisture content and volatile matters are gone and the next step is to measure the mass of fixed carbon content. Oxygen is used for fixed carbon burn off while the temperature comes down to 600 °C. Afterwards, the system asks to uncover the crucibles again to finish with the ash content analysis. Calculations for results are as follows:

Moisture-Test Method ASTM D3173

Baking oven temperature is between 104-110 °C and the particle size of the analysis sample is less than 250 micrometers.

$$Moisture = \frac{weight\ of\ used\ sample - Weight\ of\ sample\ after\ heating}{weight\ of\ used\ sample}\ 100\%\quad (3.\ 21)$$

Ash-Test Method ASTM D3174

The furnace temperature goes up to 750 °C for coal and 950 °C for coke and stays at the final temperature for about two hours.

$$As\ = \frac{Weight\ of\ full\ capsule - Weight\ of\ empty\ capsule}{Weight\ of\ analysis\ sample\ used}\ 100\%\quad (3.\ 22)$$

Volatile Matter-Test Method ASTM 3175

Furnace is preheated to 950 °C and the samples in the crucibles are heated for exactly 7 minutes. After the samples are cooled down to room temperature, they are weighed.

$$Weig\ t\ Loss = \frac{Weight\ of\ used\ sample - Weight\ of\ sample\ after\ heating}{weight\ of\ used\ sample}\ 100\quad (3.\ 23)$$

$$Volatile\ Matter = Weig\ t\ Loss\quad Moisture\quad (3.\ 24)$$

Fixed Carbon:

$$Fixed\ Carbon = 100\%\quad (Moisture + As\ + Volatile\ Matter)\quad (3.\ 25)$$

Table 9 summarizes the proximate analysis for gasified coal samples, which were used to adsorb CO_2, and Table 10 shows proximate, ultimate, and petrographic analysis of the raw coal.

Table 9 Gasified coal sample characterization

Parameter	Gasified coal samples						
	Sample 1	Sample 2	Sample 3	Sample 4	Sample 5	Sample 6	Average

Moisture	2.535	2.96	2.895	3.355	3.18	3.44	3.1
Volatile	23.23	28.4	27.04	30.5	27.875	31.57	28.1
Ash	15.125	14.43	13.195	10.24	12.895	12.185	13
Fixed C	60.645	55.86	58.56	57.84	57.89	54.23	57.5

Table 10 *Raw coal sample characterization*

Raw Coal Analysis				
Proximate analysis				
Moisture	*Volatile*	*ash*	*Fixed carbon*	
6.785	*33.72*	*5.365*	*58.07*	
Ultimate analysis				
Sulphur	*Hydrogen*	*carbon*	*Nitrogen*	*Oxygen*
0.6	*4.7*	*74.8*	*1.3*	*18.6*
Petrographic analysis				
vitrinite	*inertinite*	*liptinite*	*Maximum vitrinite reflectance*	
65.2	*22.1*	*2.1*	*0.6*	

TGA and DTG graph

The weight loss versus temperature graph captures the points at which the substance loses a component, and is generated using TGA/DSC 1 apparatus. For each experiment, about 20 milligrams of the sample is placed into the TGA pan. The first stage is called the dynamic segment, at which the temperature starts from 25 °C and rises at the heating rate of 5 °C /min until it reaches 120 °C. Then the isotherm segment starts and the temperature is kept at 120 °C for 20 minutes. Another dynamic segment continues up to the temperature of 900 °C with the

heating rate of 3°C /min. Nitrogen is used as all the segments' gas during the experiment. Table 11 and 12 show the apparatus and experiment's detail.

Table 11 *TGA apparatus specifications*

Name of the instrument	TGA/DSC 1
Model	STAR System
Manufacturer	Mettler Toledo
Probe gas	Nitrogen

Table 12 *TGA experiment plan*

Dynamic segment 1		Isotherm segment 2		Dynamic segment 3	
Start Temperature	25 °C	End Temperature	120 °C	Start Temperature	120 °C
End Temperature	120 °C			End Temperature	900 °C
Heating Rate	5°C /min	Time Iso	20 min	Heating Rate	3 °C /min

3.7　Surface area and pore volume determination

The surface area and pore volume of the gasified coal samples were measured using a Quantachrome Autosorb iQ instrument designed for surface area and pore size distribution analysis. Two different sets of experiments were run for comparison and validation. In the first series of experiments, liquid nitrogen at 77 K was used as the probe gas for initial surface area and pore volume determination. About 1 gram of the sample was ground, sieved, inserted into a 9 mm glass cell, and weighed. Each sample is weighed three times and the calculated average

weight is used as the Weight before Degassing. Samples are sent to the degas station and placed into a heat mantle. Samples were heated up to 250 °C at a ramp rate of 5°C /min with a back fill pressure of 760 torr and soaked for four hours. Once the outgas stage is done, the sample is weighed again to record the Weight after Degassing and sent to the sample station with a dewar flask filled with liquid nitrogen. A 20-point preset program was used for the surface analyzing experiment, and results were analyzed with the DFT method and the multipoint BET equation. Another set of tests were run using CO_2 as the probe gas at 0 °C. In this case, the 3-liter dewar flask for analysis is filled with cold water and ice cubes to keep the temperature at 0 °C during the experiment. The outgas temperature was 350 °C at a ramp rate of 5°C /min with a back fill pressure of 780 and a soak time of 5 hours. Table 14 shows the experiment condition of nitrogen surface analyzer along with CO_2 surface analyzer tests.

Table 13 *specifications of the surface area and pore size distribution analyzer*

Name of the instrument	Automated Surface Area and Pore Size Analyzer
Model	Autosorb iQ (ASQ)
Manufacturer	Quantachrome Instrument
Probe gas	CO_2 and N_2

Table 14 *Pore Volume experiment's condition*

Test name	Surface Analyzer	
Used Gas	N_2	CO_2
Pressure Point Counts	20	20
Outgas Temperature	250 °C	350°C
Outgas Time	4.7 hrs	5 hrs
Cell Type	9 mm WoR	6 mm WoR

Chapter 4

4 Results and Discussion

In this research, four separate experiments have been conducted on coal: thermogravimetric analysis on raw, gasified, and CO_2 adsorbed coal, surface analyzer test on raw and gasified coals, image analyzing test on raw and gasified coal, and volumetric adsorption on gasified coal. Each experiment had its own way of sample preparation, which was explained, comprehensively, in the experimental section of this thesis.

Raw Coal		
TGA	BET	SEM

6 Gasified Coal + 1 Ash			
TGA	BET	SEM	Volumetric adsorption

CO_2 Adsorbed Coal
TGA
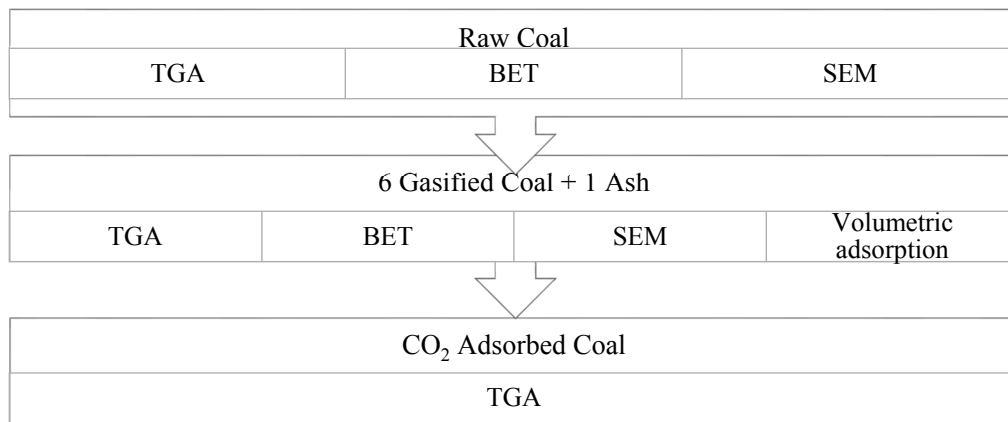
Figure 17 Experiments associated with each stage of coal sample

The main purpose of the study is to quantify the adsorption amount of carbon dioxide onto gasified coal parts from the underground coal gasification process toward CO_2 capturing and storage (CCS) fulfillment. Experiments are conducted at 45.5 °C and pressures from 500 Psia up to 1000 Psia. Supercritical measurement was also done for two of the samples to show the fluid behavior of CO_2 once injected into a porous solid.

Ahead of the adsorption measurement experiments, coal's physical properties such as pore size distribution and total pore volume are required for a better understanding of the adsorption

behavior. Nitrogen and carbon dioxide BET tests, also known as surface analyzer experiments, were employed to provide pore volume and pore size distribution of the gasified samples. More importantly, these experiments provide the surface area of the samples, which is considered a beneficial tool for adsorption behavior analysis of porous solids.

Proximate analysis of samples is also required to examine the effects of different compounds such as moisture, volatile, fixed carbon, and ash on the adsorption amount of gasified coal. It can also be implied through the proximate analysis of samples, how the gasification process alters coal composition. The TGA apparatus was used to probe the percentage of compounds in coal samples and the results are discussed below. The TGA DSC 1 apparatus provides mass loss per time graphs, which are employed to make a comparison between raw coal samples, and adsorbed ones. These graphs are helpful in capturing changes occurred during the volumetric adsorption process.
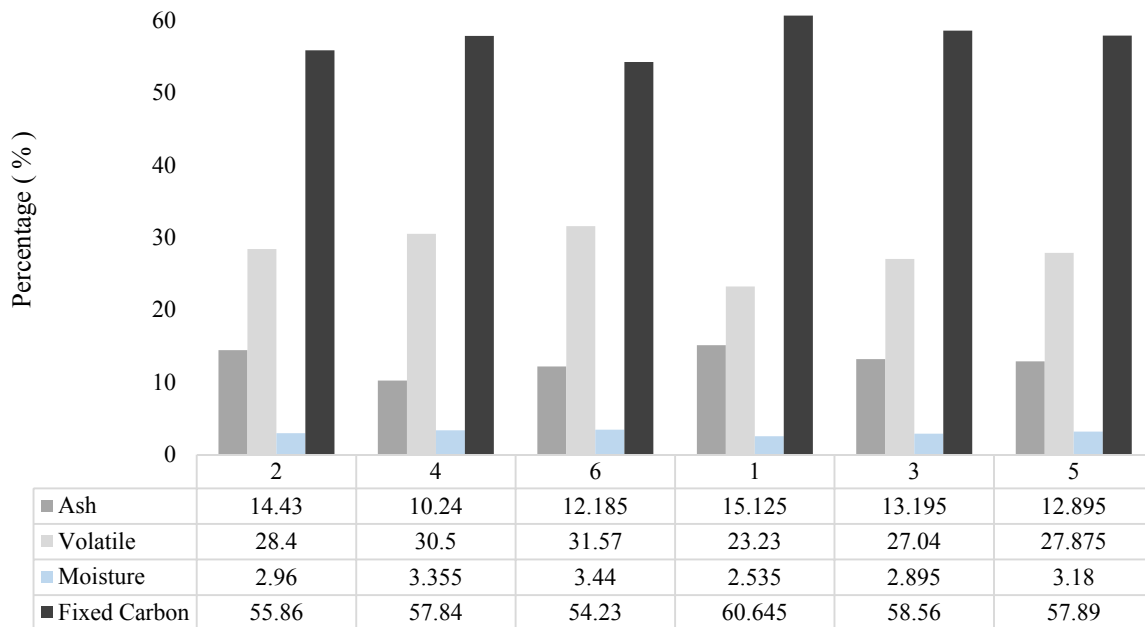
4.1   TGA result of raw coal and gasified coal

Once coal is gasified during the UCG process, its compounds' percentage changes and either develops the structure for a better adsorption environment or blocks some of the pores and destroys others. Two different thermogravimetric analyses were engaged to see the compounds' change in the samples before and after gasification and how they are vaporized over time while temperature rises. The first TGA experiment gives the proximate analysis of six gasified samples representing their moisture, ash, volatile, and fixed carbon contents. The latter analysis provides a graph of sample weight loss versus time or temperature based on the boiling points of decomposing compounds.

4.1.1 Proximate analysis

Figure 18 shows the proximate analysis of six gasified samples taken from the UCG process. It can be seen from this figure that all samples have approximately 60 percent of fixed carbon and


	2	4	6	1	3	5
■ Ash	14.43	10.24	12.185	15.125	13.195	12.895
▪ Volatile	28.4	30.5	31.57	23.23	27.04	27.875
▪ Moisture	2.96	3.355	3.44	2.535	2.895	3.18
■ Fixed Carbon	55.86	57.84	54.23	60.645	58.56	57.89

Figure 18 *Proximate analysis of gasified coal samples*

30 percent of volatile matter. Moisture content is minimal because of exposure to high temperature during the gasification process.

However, this figure alone cannot illustrate what actually occurred in the gasification process and thus a comparison between raw and gasified coal content is required. In this regard, two raw coal samples, each weighing 2 grams, were tested for their proximate analysis and results were averaged and compared with the gasified samples' average values (See figure 19).

Figure 19 clarifies the difference between the compounds' contents before and after gasification process. As shown in figure 19, moisture and volatile contents of samples have decreased. Ash is a solid residue, which is left after coal combustion and consists of heat-treated mineral matter (inorganic constituent) such as metal oxides, arsenic, and mercury (89).
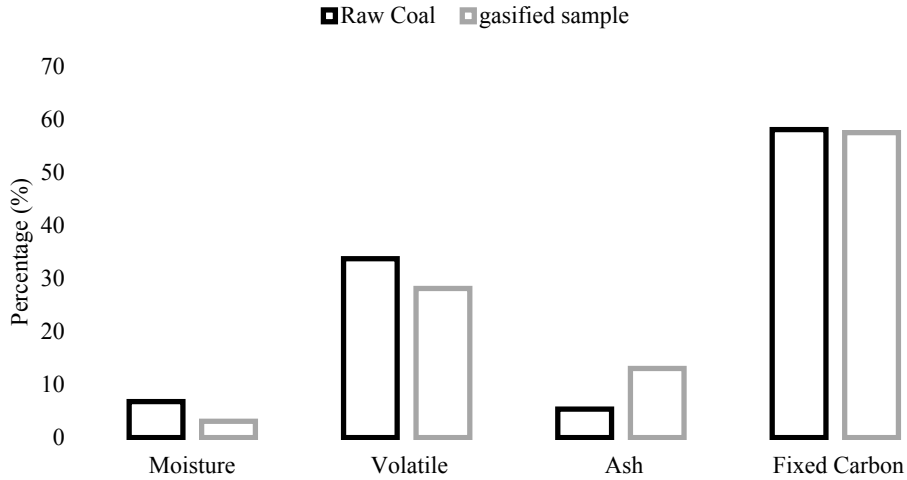
Figure 19 *Comparison of Proximate Analysis of raw and gasified Coal*

A various range of ash-forming compounds is scattered throughout coal which also varies in concentration from part per million to per cent (90). By definition, the amount of ash content before and after the gasification process should be similar.

By comparison between the fraction of ash content before and after gasification, the conversion ratio, X (%), of raw coal (take W_0 as mass of raw coal sample) to gasified coal (W) can be obtained.

$$X \ (\%) = \frac{W_0 - W}{W_0} \times 100$$

In this study, average ash content fraction to total mass of sample, according to the proximate analysis, has changed from 5% to 13% before (Y_{ash_0}) and after (Y_{ash}) the gasification process respectively:

$$X \ (\%) = \frac{Y_{ash} \quad Y_{ash_0}}{Y_{ash}} \quad 100$$

Using the equation above, 58.8% is obtained for average conversion ratio of raw coal to gasified coal. Adopting this conversion ratio gives real masses of moisture, volatile, ash, and fixed carbon contents in gasified coal while keeping ash amount at a constant value. Table 15 summarizes the conversion factor for all six coal samples. Figure 21 illustrates changes in fixed carbon of samples before and after gasification.

***Table 15*** *Conversion ratio of samples*

Sample ID	Conversion Rate (%)
1	64.5
2	62.8
3	59.3
4	47.6
5	58.4
6	55.9
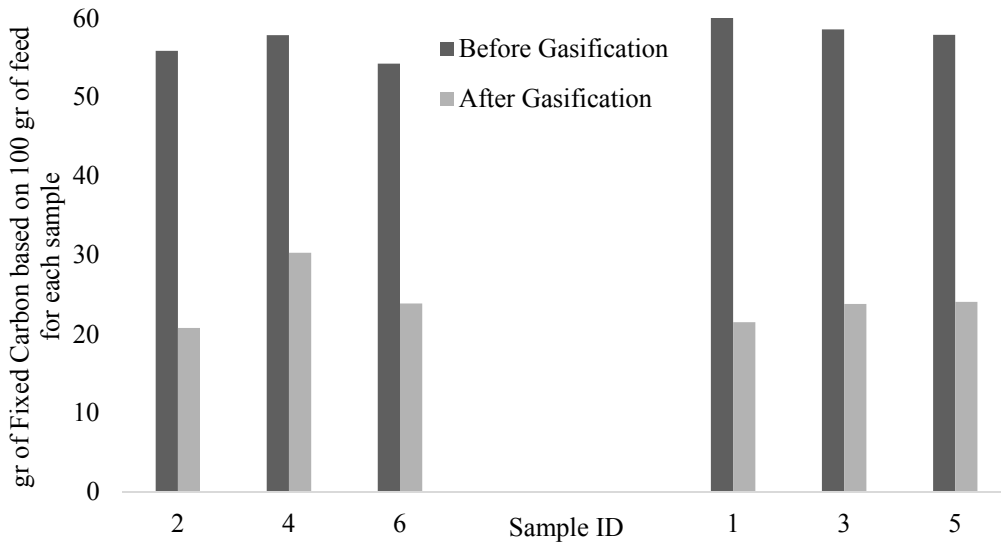
Figure 20 *Carbon conversion values during the gasification*

Figure 20 represents carbon content of Region 1 (left side of the graph) and Region 2 (right side in the graph). Region 2 shows lower carbon content overall, after gasification which is a sign of more alteration during UCG. Pore volume and surface area measurements in the next section also prove this statement.

Employing conversion rates from Table 15 will give the amount of remaining carbon in samples after gasification process. Comparing the amount of fixed carbon in gasified samples with raw samples illustrates, alteration of all compounds throughout the gasification. Figure 21 shows a graph of proximate analysis of coal before and after the gasification with the vertical axis representing mass of compounds on 100 grams of basis. It gives a clear understanding of what changed during the gasification process. According to the graph, moisture and volatile contents of coal has decreased by 80 % and 65% respectively. Ash content is constant due to ash definition and fixed carbon has decreased 58% by reason of converting to syngas.
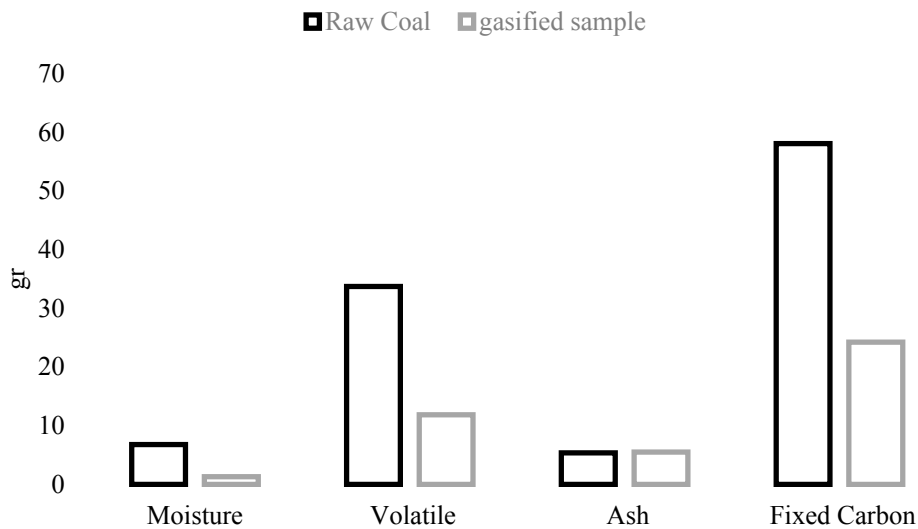

Figure 21 *Normalized proximate analysis of raw and gasified coal*

4.1.2 TGA and Derivative TGA

This type of TGA experiment was conducted to compare coal samples before and after adsorption of CO_2. Thermal analysis methods allow the investigation of all chemical processes associated with heating and cooling. Processes include decomposition, pyrolysis, ignition, phase change, etc. the simplest analysis is TGA in which samples are mechanically connected to an analytical balance assembled around a furnace and records mass change versus temperature or time. In case of coal analysis, the sample is heated in nitrogen to evacuate any volatiles and thereafter sample environment changes to oxygen to burn carbon in coal to CO_2. Weight loss in this step is used to measure carbon content of the sample. It is a very practical approach to take the first derivative of the TGA curve, known as DTG, as it captures small features and changes in TGA and represents them as peaks in the curve. DTG curve is a plot of the rate of change of mass with respect to time.
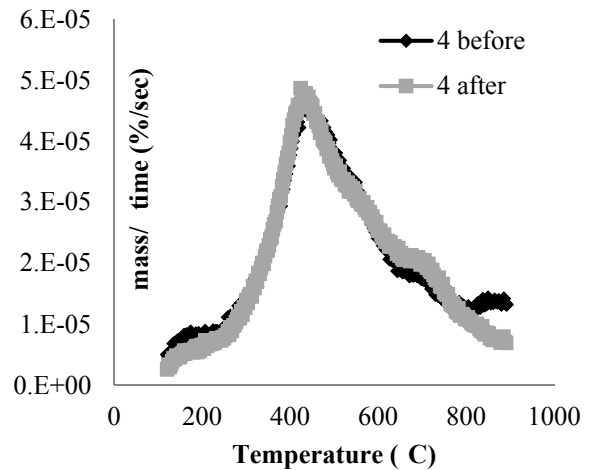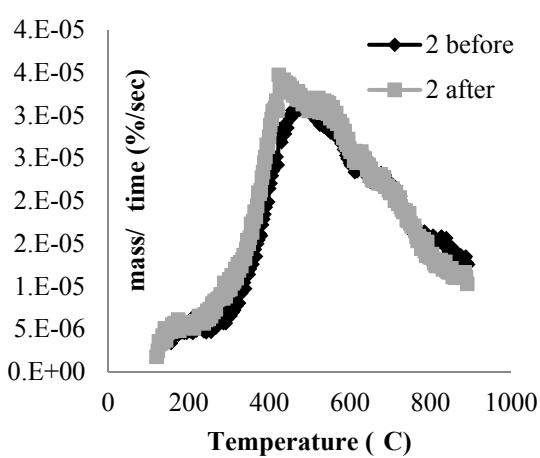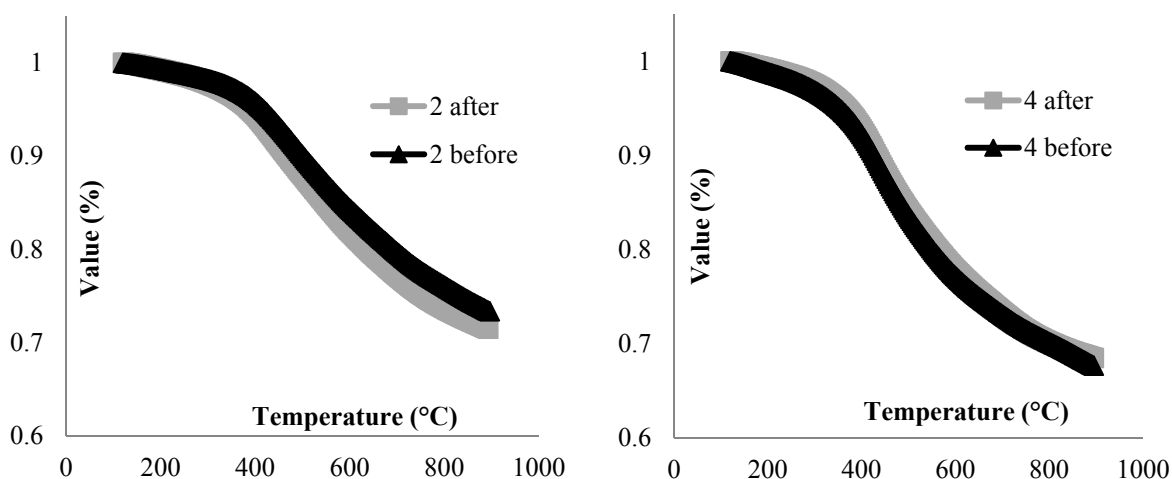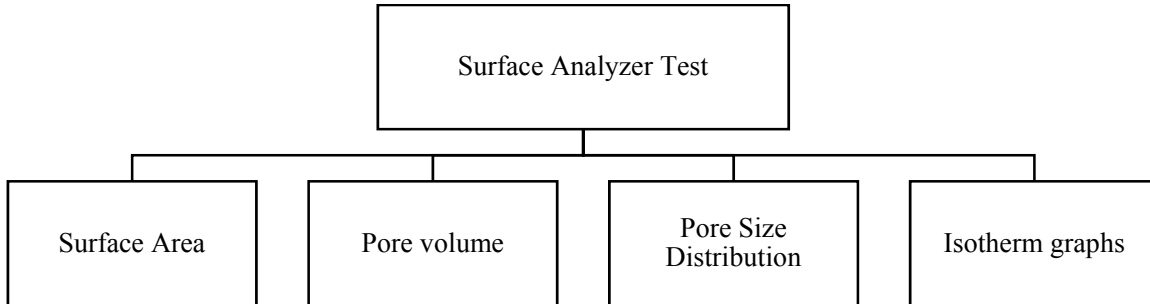
Figure 22 *DTG and TGA analysis of samples before and after CO_2 adsorption*

Illustration can be made on the type of adsorption (physical or chemical) through analysis of TGA and differential TGA (DTG) graphs. DTG and TGA graphs of two samples are shown in figure 22. DTG plots are generated by computing the derivative of the graph of mass loss versus temperature. Overlap of the graphs before and after adsorption indicates physical sorption of carbon dioxide on coal, which is in agreement with the literature (7). When taking CO_2 adsorbed samples out of the volumetric adsorption setup, pressure is removed leaving samples at atmospheric pressure. Adsorption onto coal occurred when pressure was applied gradually to the system. Now that the pressure is released, CO_2 has come out of the pores representing a physical adsorption according to DTG and TGA graphs. Therefore, coal before and after adsorption process is showing the same peaks in its DTG graph, rejecting any chemical reaction occurrence in itself.

4.2   Adsorption analysis

Two separate sets of experiments were run with Quanta chrome surface analyzer using N_2 and CO_2 as probe gases. The generated outputs from these series of experiments are sketched in figure 23. Discussion and explanation of each result will be made in the following sections.

```
                    ┌─────────────────────────┐
                    │   Surface Analyzer Test  │
                    └─────────────────────────┘
        ┌──────────────┬──────────┴──────────┬──────────────┐
  ┌───────────┐  ┌───────────┐  ┌──────────────┐  ┌──────────────┐
  │ Surface   │  │   Pore    │  │  Pore Size   │  │   Isotherm   │
  │   Area    │  │  volume   │  │ Distribution │  │    graphs    │
  └───────────┘  └───────────┘  └──────────────┘  └──────────────┘
```

Figure 23 Surface and pore volume analyzer test outputs

4.2.1 Adsorption isotherms

The adsorption process is normally evaluated through graphs known as Isotherm graphs. It is a graph based on the volume of adsorbate adsorbed onto the surface of adsorbent with respect to relative pressure, which is equilibrium pressure divided by saturation pressure. Equilibrium pressure is defined as vapor pressure above the sample corrected for the desired temperature, and saturation pressure is vapor pressure above a liquid. CO_2 vapor pressure is 26141 torr, which is set as P_0 in isotherm graph. Isotherm graphs of six gasified samples, raw coal, and coal ash sample in CO_2 experiments are presented below (figure 24). Sample 3 and Sample 1 located at the center and bottom of the coal core (figure 10) are showing the highest adsorption volume. The coal ash results showed that it does not hold any storage capacity in itself. Raw coal is showing the lowest adsorption isotherm after coal ash. This is a good indication, which shows

UCG has helped coal to develop more pore volume and surface area for more adsorption capacity.
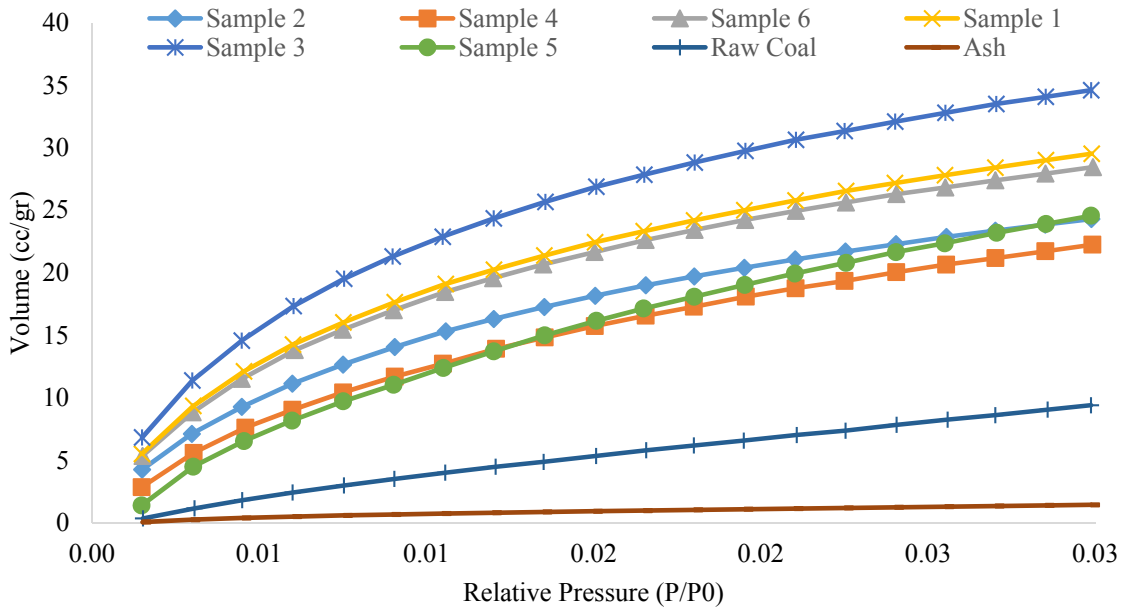
Figure 24 *Adsorption isotherms of CO₂ at 273K and atmospheric pressure*

Adsorption isotherm graphs need some characterizations such as pore volume, pore size distribution, surface area, and average pore size. A more detailed investigation of outputs and particularized results are discussed in subsequent sections.
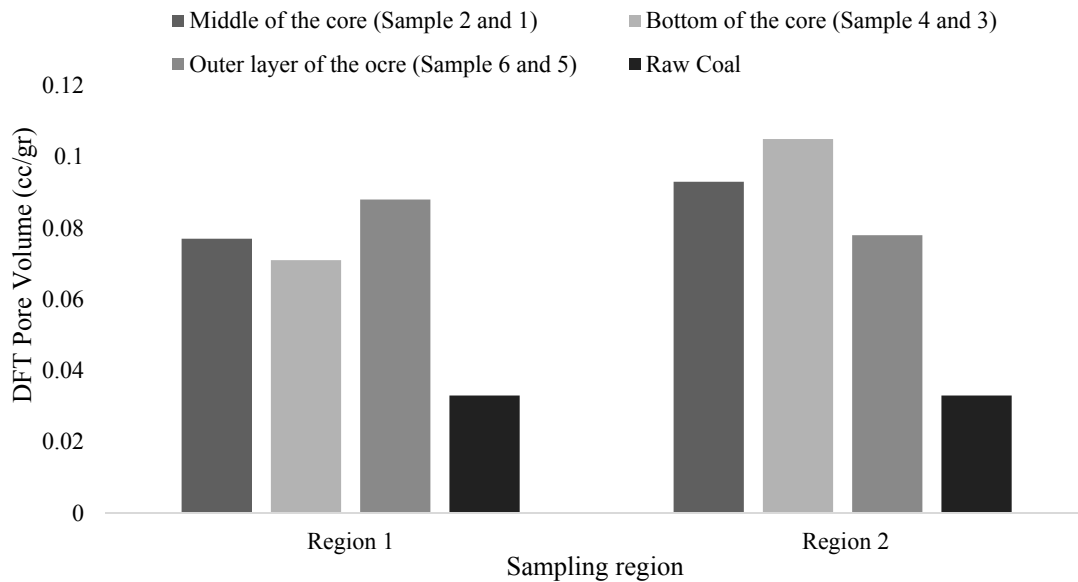
4.3 Pore volume

One of the features of isotherm graphs is that the pore volume of samples can be determined using any of the analysis methods available in the software. The pore volume of gasified coal samples was determined using nitrogen and carbon dioxide surface area tests adopting DFT model. Table 16 shows pore volume of samples obtained from nitrogen and carbon dioxide surface analyzer tests.

Table 16 *Pore volume of coal samples from N₂ and CO₂ tests*

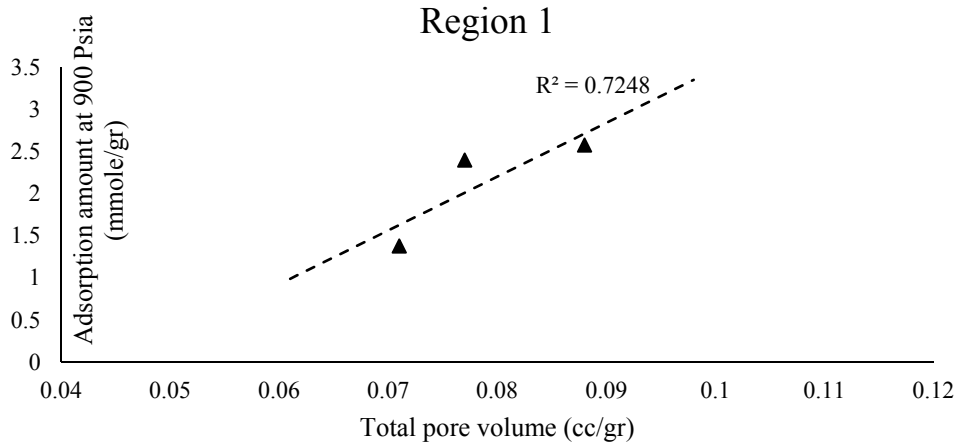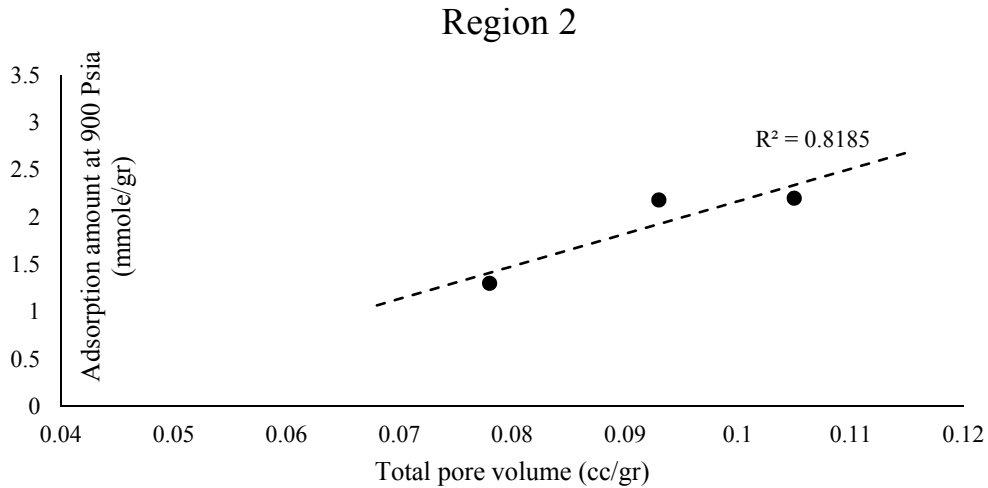| Sample ID	Total Pore Volume (cc/gr)	
	Nitrogen	CO$_2$
Raw Coal	-	0.033
1	0.181	0.093
2	0.125	0.077
3	0.181	0.105
4	0.0645	0.071
5	0.032	0.078
6	0.416	0.088

To emphasize how pore volume has changed and increased during the gasification, pore volume of raw coal was measured with DFT method in surface analyzer tests and compared with gasified coal's pore volumes. The samples are grouped into their respective region and each region's property is compared with raw coal's property. Figure 25 shows the pore volume development during the gasification of coal. The samples in Region 2 have more pore volume compared to Region 1 samples. Sample 3 in Region 2 has the highest pore volume in this experiment (0.1 cc/gr) as expected from its adsorption isotherm in figure 24. Sample 4 has the lowest pore volume among others. It is clearly noticeable that the overall pore volume has increased over three times. There is not any distinct relation between the pore volume values of different positions in coal, which could be due to a nonlinear gasification path.

Figure 25 *Pore Volume development after gasification*

According to Table 16, nitrogen tests indicate larger average pore volume as nitrogen molecules penetrate larger pores in coal. Sample 4 shows the smallest pore volume in both tests; however, as mentioned earlier, the characteristics of the samples are very alike and a one-by-one comparison is not the best solution for data analysis. Therefore, a graph of adsorption amount versus total pore volume for each sampling region is provided to inspect any relation between coal porosity and adsorption capacity of different regions. Figure 26 shows the adsorption capacities of the samples at 45.5 °C and 900 Psia with respect to total pore volumes obtained from CO_2 surface analyzer tests. The horizontal and vertical axes are scaled similarly to help graph comparison.

The CO_2 adsorption on gasified coal at high pressure is not a monolayer adsorption phenomenon, and adsorbate's molecules stick to each other and to the surface of the pores in the form of multilayer adsorption; thus, the value of the total pore volume is of interest in this study.
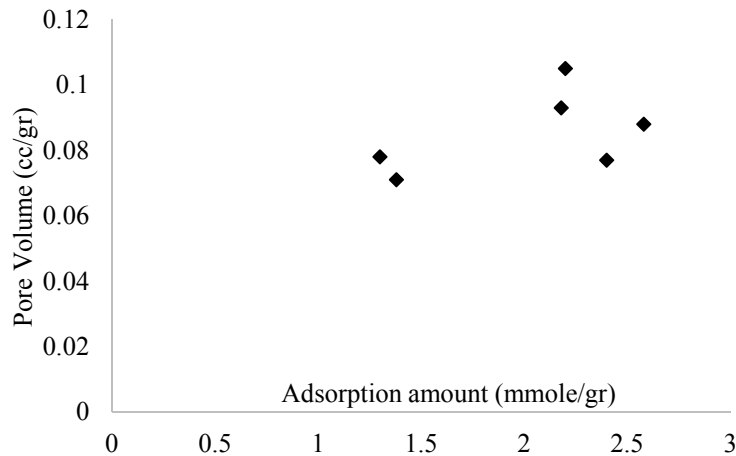
Figure 26 *Effect of total pore volume on CO₂ adsorption capacity*

Both regions show a linear relationship between the adsorption capacity and pore volume of samples. As discussed earlier, CO_2 molecules adsorb on the surface of the adsorbent in multilayers form and can fill up the total pore volume if required conditions are provided. This linear trend confirms the multilayer adsorption of carbon dioxide in coal. The samples in Region 1 have closer values of pore volumes that result in a higher slope for the linear line. In Region

2, the adsorption capacities of the samples are closer to each other and pore volumes are more widely distributed and contain higher values.

It should be noted that pore volumes used in graph 26 are obtained from CO_2 surface analyzer tests, which could only observe micropore volumes. It is expected that higher pore volumes attract higher amount of adsorbates' molecules so if larger pores have been taken into consideration in these experiments, higher adsorption capacity would have been noticed. If considering all samples in one graph regardless of their region, figure 27 is achieved. It shows adsorption values of all samples at 900 Psia and 45 °C. Sample 4 and 5 have the lowest
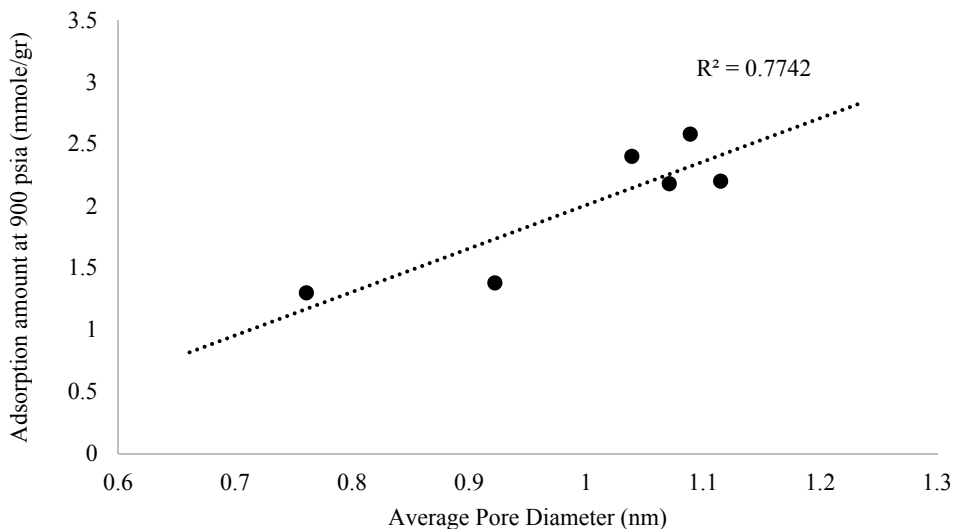

Figure 27 *Effect of pore volume on CO_2 adsorption capacity*

adsorption capacity and consequently lowest pore volumes as they also had the lowest adsorption isotherms among other samples. All other samples have almost similar values in big scale. Basically, figure 27 confirms that more pore volume yields more adsorption capacity regardless of sample positioning.

It was of interest to investigate the effect of average pore size of gasified coal samples on their adsorption capacity. According to figure 28, total adsorption capacity increases linearly as

average pore size increases. According to the literature, there is a strong relationship between

Figure 28 *Effect of average pore size on CO2 adsorption capacity*

micropore volume and adsorption capacity of adsorbents (91, 92). In this study, average pore volumes are within micropore range and confirm findings in the literature.
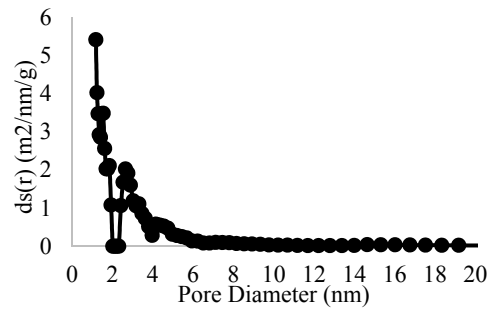
4.4 Pore size distribution

The pore size distribution of gasified coal samples has been retrieved by DFT analysis of adsorption isotherms of CO_2 and N_2. To see the contribution of different pore sizes to total surface area, graphs in figure 29 are generated using values extracted from the DFT pore size distribution model. Two separate graphs are provided for each sample, one comes from the CO_2 test representing only pores up to 1.5 nanometer in diameter, and the next graph comes from the N_2 test, which exhibits pore size distribution of pores larger than 1.5 nanometer in diameter. Digit orders in the CO_2 test graphs are much higher than those in the nitrogen graphs. The reason is that CO_2 captures micropores, and micropores have much more surface area in themselves rather than meso- and macro- pores. The graphs together give an overall

understanding of pore size contribution of the samples to their total surface area. In all gasified

samples, pores with 0.5 nm diameter contribute effectively to the surface area of the coal. This

contribution can be noticed from a sharp rise in dS(r) versus pore size graphs in which S is the

surface area of samples and r is half pore widths. This decreases as pore size increases

thereafter. The next noticeable contribution is related to mesopores of sizes 2nm to 3nm.

Samples 2, 4, and 5 are also representing another peak at around 15 nanometers. The graphs

from nitrogen and carbon dioxide tests cannot be put together and compared. However, having

them next to each other can provide a better insight about total pore size distribution in the
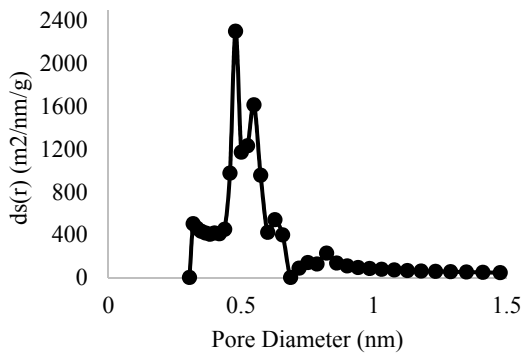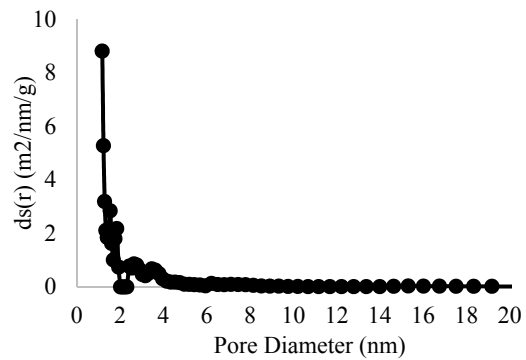
samples.

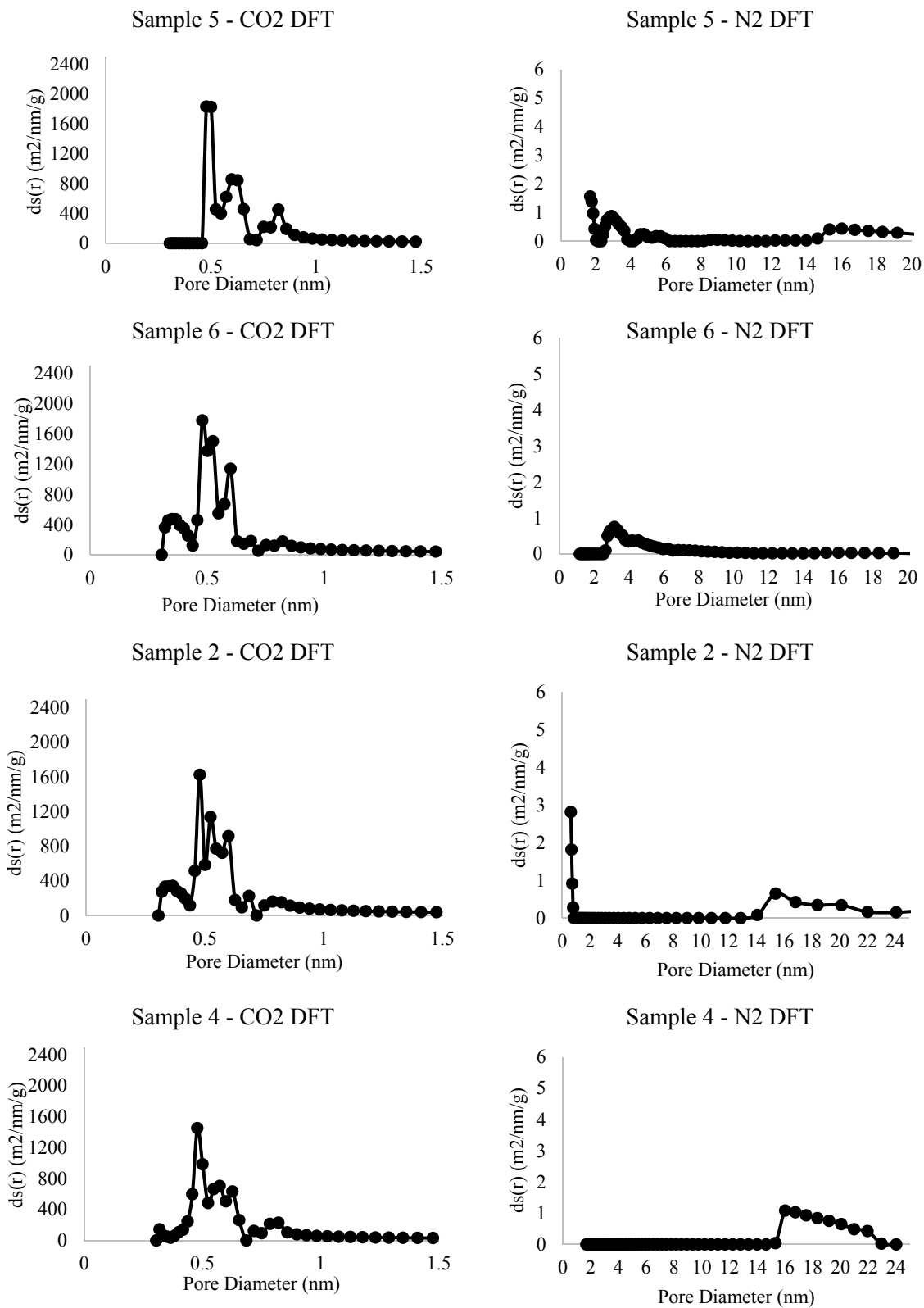Sample 1- CO2 DFT
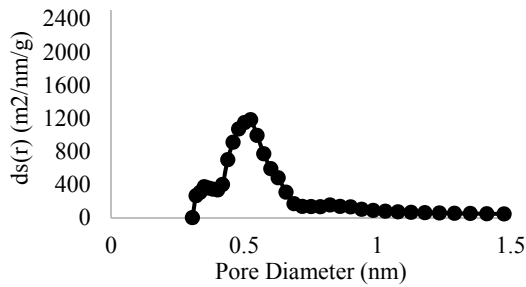
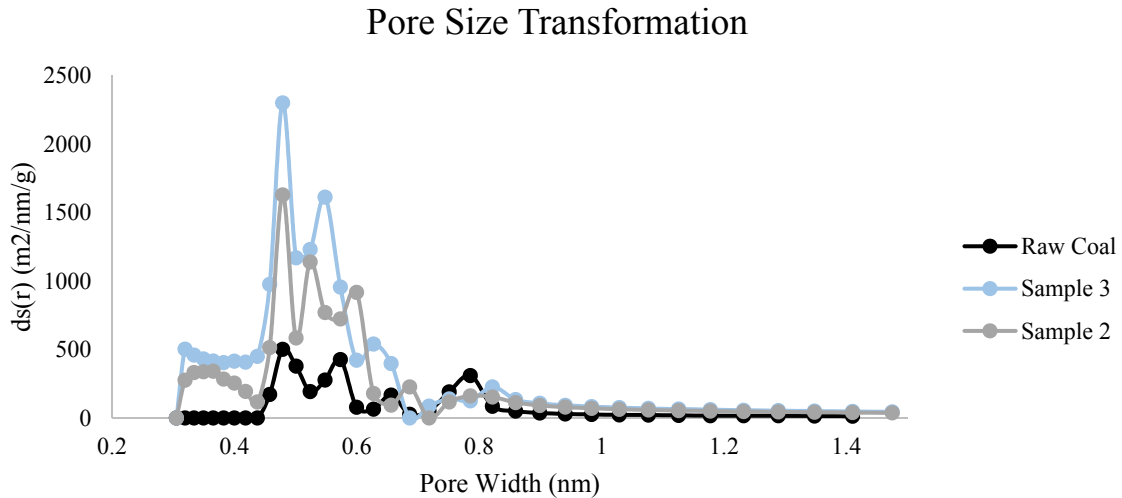Sample 1- N2 DFT

Sample 3 - CO2 DFT

Sample 3 - N2 DFT

Figure 29 *Pore size distribution and its contribution to total surface area*

The pore size distribution of raw coal and two of the samples are plotted in the same graph to observe the pore size transformation during the UCG, and how it contributes to the total surface area.

Pore Size Transformation

Figure 30 *Effect of gasification on pore size distribution of the coal and the contribution of pore sizes to the surface area*

4.5   Surface area

Surface area and porosity are leading factors in adsorption studies. Surface area for gasified coal samples is obtained from DFT analysis method in surface analyzing experiments with CO_2. For a clear understanding of surface area development during UCG, surface areas of samples from Region 1 and Region 2 are compared with raw coal surface area in figure 30. It can be seen from figure 30 that samples from Region 2 have developed more surface area during the underground coal gasification process mainly due to micropore growth. Sample 3 has the highest surface area among other samples and is the one that had the highest pore volume and adsorption isotherm. In general, the samples from six different locations on the coal core have expanded up to three times their original surface area. It is not easy to find a relationship

69

between surface area developments of samples and their regions. For example, in Region 1, the surface area of Sample 6 located at the outer layer of the core has increased more than the other samples and in Region 2, Sample 3 located at the bottom of the core is holding the highest surface area.
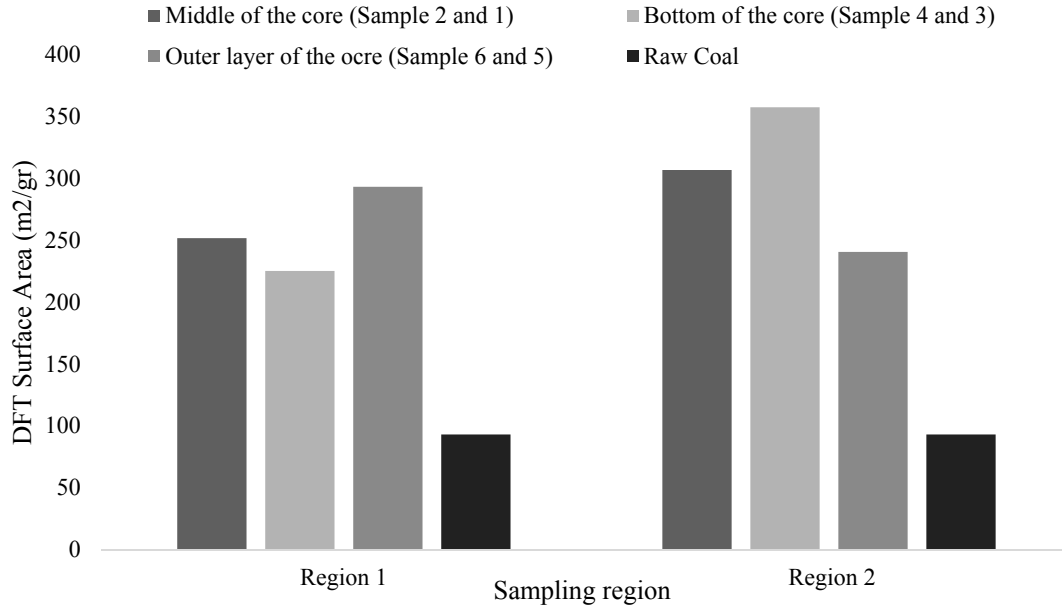
Figure 31 Surface area development during gasification

Effect of surface area on adsorption capacity of the samples is also investigated. The samples are divided into two regions and plotted separately with respect to their adsorption capacity, from the volumetric setup adsorption measurement at 900 Psia and 45 C. The plots are scaled similarly to allow for easier one by one comparison. As shown in figure 31, higher surface area leads to higher adsorption capacity in a liner manner. The adsorbate's molecules can fill all the surface area available with the adsorbent and repeat the adsorption process in multi layers. In addition, the samples of Region 2 cover a wider range of surface area in comparison with the Region 1 samples. This was also observed in the pore volume graphs. Samples from Region 2 had more pore volume and they now reveal more surface area. The largest observed surface

area from the DFT method is 357 m2/g, which belongs to Sample 3, and the lowest surface area comes from Sample 4 valued at 225 m2/g.
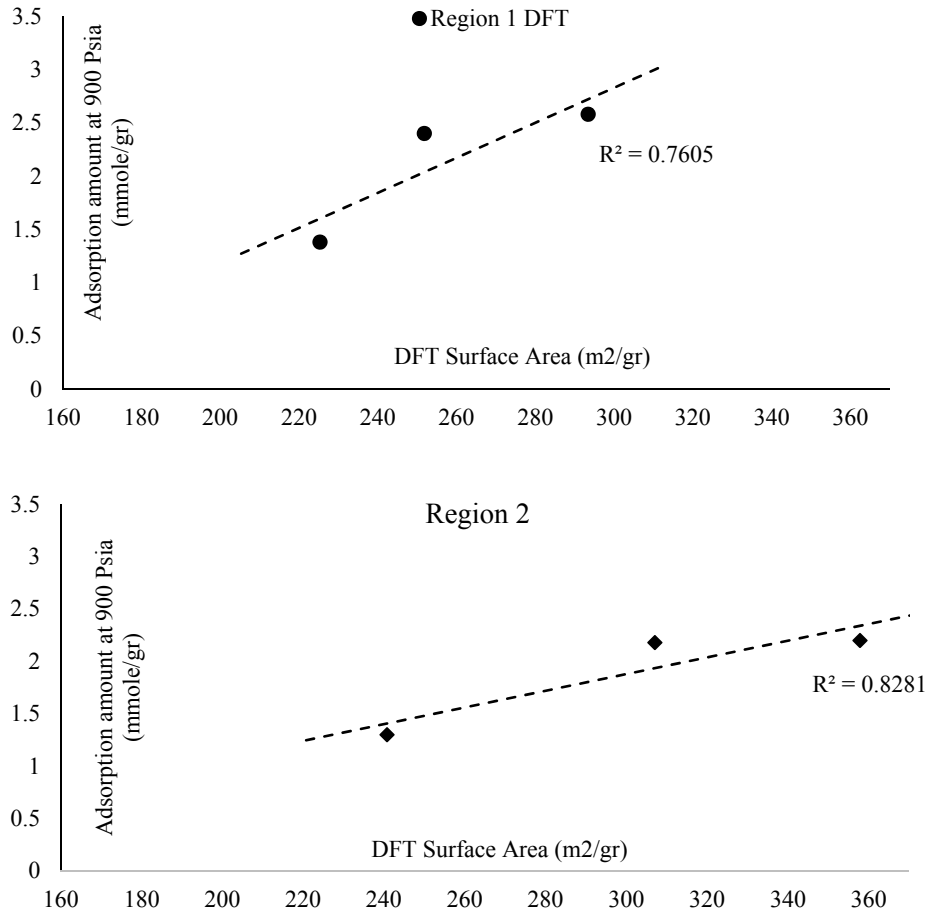
Figure 32 Effect of surface area on CO_2 adsorption capacity

DFT surface area for raw subbituminous Canadian coal is measured around 90 m2/g. The development of surface area in gasified coal samples in this study is the result of enlarged pores due to coal decomposition and gasification at high temperatures. Decompositions cause micropores to form in the coal structure leading to excess surface area for CO_2 adsorption.

4.6　Adsorption capacity measurement

Adsorption values reported in this section are excess adsorption values calculated from Gibbs excess adsorption equations. The isotherm graphs of six gasified samples are presented in figure 33.
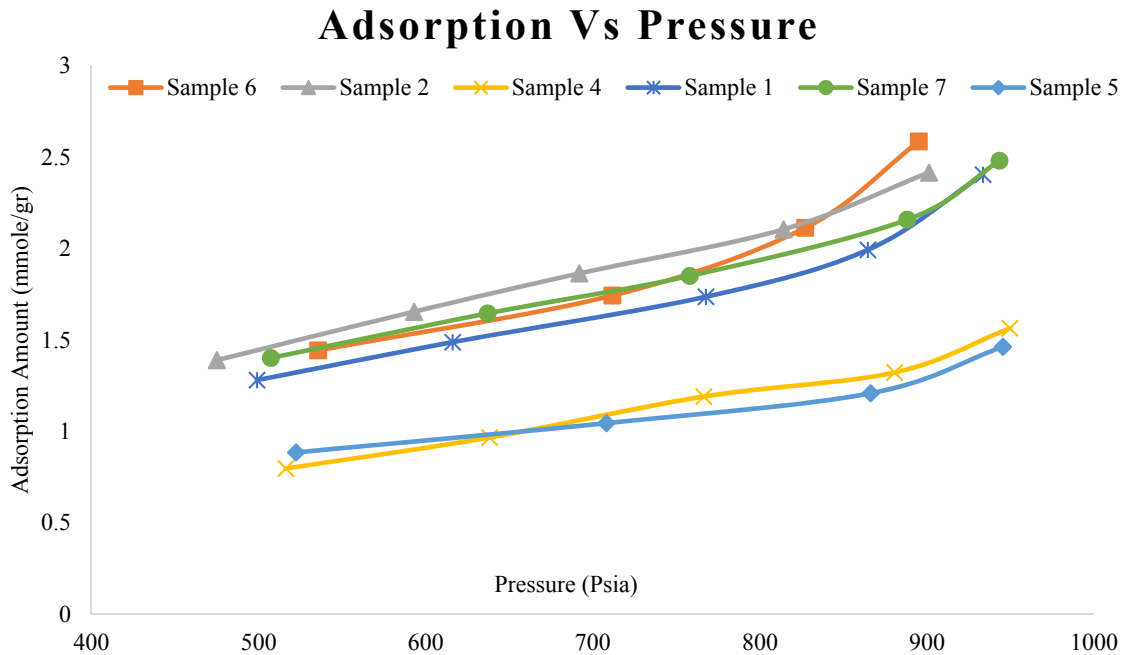
Figure 33 *Adsorption isotherm of CO_2 on gasified coal at 45.5 °C extracted from the volumetric adsorption setup*

The volumetric setup adsorption isotherm is closely in agreement with the CO_2 adsorption isotherm from the surface analyzer experiment. Adsorption of samples at fixed temperature of 45.5 °C and pressure range of 500 Psia to 1000 Psia are measured. Among all samples, Samples 4 and 5 show the lowest values for their adsorption capacities. Samples 3, 1, 2, and 6 have higher adsorption capacities but not in the same order as their isotherm results from surface analyzer tests. However, samples 3, 1, and 6 show the same trend as figure 27. The maximum adsorption capacity from volumetric adsorption setup is related to Sample 6 at 900 Psia with an

amount of 2.58 mmole/gr, and the minimum capacity is for Sample 4 at 516 Psia with an amount of 0.79 mmole/gr.

Additionally, all samples show a steady increase in adsorption while pressure increases until about 850 Psia and continues with a higher slope afterward. The last pressure point for these experiments were chosen below 1000 Psia as the critical pressure of CO_2 is 1071 Psi, and CO_2 will behave differently once it changes to fluid. The overcritical measurement and its results are discussed in the last section of this chapter. Change of the slope in the last pressure point of these isotherms is due to it being close to critical pressure of adsorbate gas. There are many overlaps in the plot as characteristics of samples are close to each other's because they have been located in the core only 2 inches apart from one another.

4.6.1 Adsorption over time

Adsorption capacities of the six gasified coal samples taken from the lab scale UCG experiment were measured adopting the volumetric adsorption setup at 45.5 C. Samples were a mix a coal chunk and powder. For each sample, five different pressure points were recorded and, for each pressure, 24 hours were passed to reach equilibrium. This practice requires nonstop work and supervision on experiments, although it provides very accurate results. In this regard, the pressure data points for every hour were extracted from the excel file of pressure recordings, substituted into adsorption calculation equations, and figure 31 was obtained. It shows adsorption versus time plot for the randomly chosen data points of the experiments.
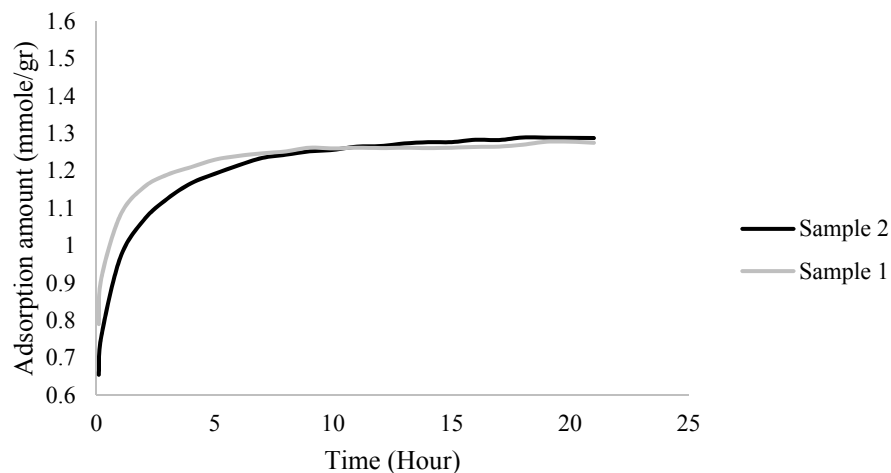
Figure 34 *Effect of equilibrium time on CO$_2$ adsorption capacity*

At the beginning of the experiment, the pressure is not yet stable and varies sharply, but as time passes the pressure in the experiment cell reaches an acceptable equilibrium, for which more wait time does not change the adsorption capacity of the samples dramatically. In this study, for all experiments, the pressure point at 20 hours was selected to calculate the adsorption capacity. It is beneficial to have a graph of adsorption capacity of a sample over time to see how much difference it makes if the pressure at 3, 5, 10, and 15 hours is taken. An adsorption values comparison at 10 hours and 20 hours for the different samples at the different pressure points is represented in figure 33. The linear relationship confirms that adsorption values for all samples at 20 hours are only 0.5 % higher than its value at 10 hours. Therefore, a lot of time can be saved by simply adding 0.5% to adsorption capacity at 10 hours to obtain capacity after 20 hours.
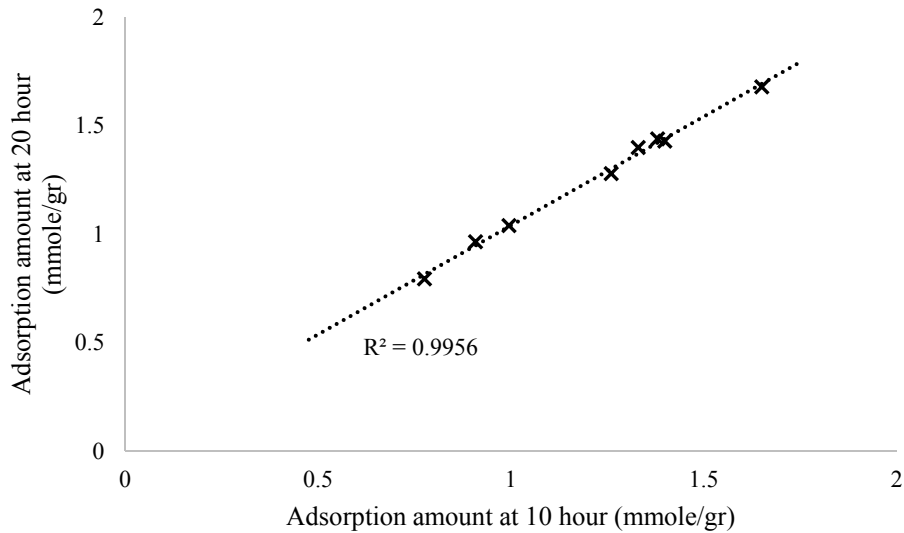
Figure 35 Comparison of adsorption values at 10 and 20 hours

4.6.2 Ash adsorption capacity

Once gasification happens, some parts of the coal convert completely to syngas and only ash particles are left in the gasification site. Therefore, a sample of mostly ash from another UCG test was taken and experimented on to measure its potential adsorption capacity, the result is shown in figure 35. The ash particles that remain from the UCG experiment have zero capacity
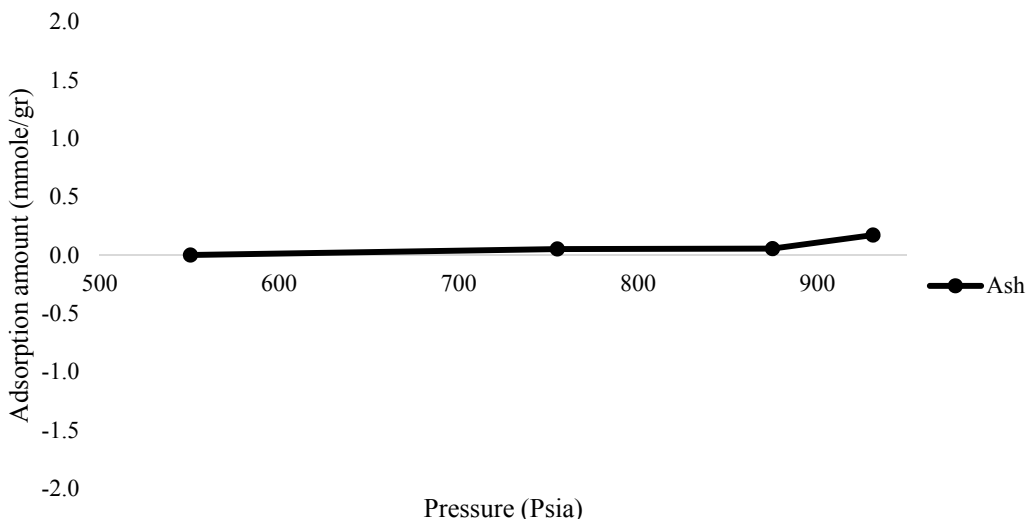
Figure 36 Adsorption capacity of CO_2 on coal ash

for carbon dioxide adsorption. The values that deviate from zero as shown in the graph are due to experiment and calculation errors.

The ash sample was also taken for a surface analyzer test and outputs are tabulated below.

Table 17 Surface area and pore volume of ash

Sample Name	Ash
DFT Surface Area (m2/gr)	15.47
Multipoint BET Surface area (m2/gr)	18.61
Total pore volume (cc/gr)	0.006

Comparing the raw coal surface area (93m2/gr) with the ash surface area (15.47m2/gr) validates the zero adsorption capacity of the ash sample in volumetric setup.

4.6.3 Super critical adsorption measurements

The pressure range for adsorption capacity measurement in this study was between 500 and 1000 Psia, which is considered high pressure but below the critical pressure of CO_2 (1071 Psia). Adsorption isotherm trends of gasified coal samples at near critical pressure were showing a different slope that urged further investigation and experiments. It was also recommended in literature that for a more specific understanding of UCG-CCS system, the experiments are required to be conducted at over critical pressures to cover a wide range of pressures (10). In this regard, two of the gasified samples were randomly chosen to be experimented in volumetric adsorption apparatus under pressures from 500 to 1500 Psia and at a temperature fixed at 45.5 °C as a representation of abandoned underground coal gasification sites. Figure 32 shows these results.

76
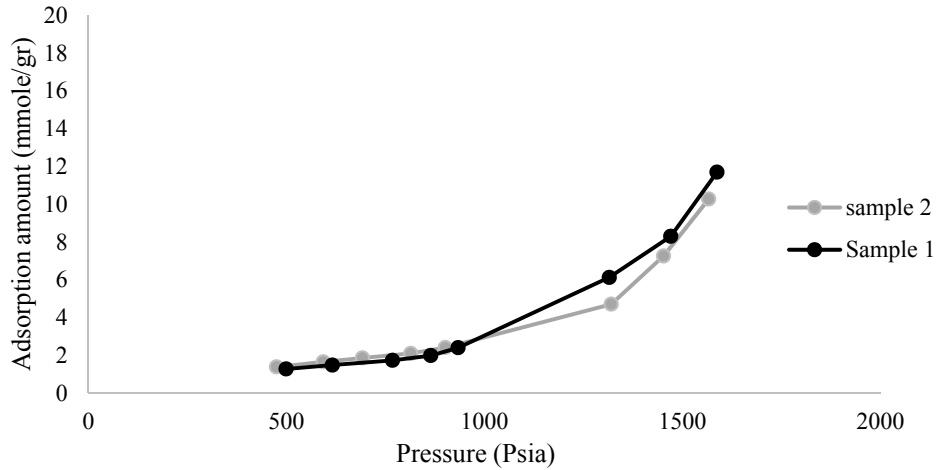
*Figure 37 Adsorption capacity of gasified coal at super-critical pressures*

It can be seen from figure 32 that after the critical pressure, adsorption capacity of coal increases almost exponentially reaching a maximum of 14 mmole/gr at 1540 Psia for Sample 2 and 13 mmole/gr at 1570 Psia for Sample 1. Results show that with pressurizing the system, the adsorption capacity of gasified samples from post UCG sites can expand up to 5 times storing more CO_2 economically. It should be noted that more pressure means more cost and the optimum pressure of CO_2 storage should be assessed economically.

4.7   SEM analysis

Six gasified coal samples and a raw coal sample were examined under a scanning electron microscope to observe structure differences in the samples. Images were taken at various magnitudes and compared with one another. The captured images were taken at the same magnification so that these images would be easy to compare; however, because of different particles heights and working distance from the microscope, Sample 2 is presented at a larger scale. Nevertheless, scaling is provided in all pictures, which makes comparison and interpretation easy. Figure 38 shows SEM images of 7 samples with raw coal on top, samples

from Region 1 in left column and samples from Region 2 in right column. It can be seen from the images that raw coal has a smoother surface, which is not much developed with fractures and pores. Sample 2, which had high adsorption capacity recorded by volumetric adsorption setup, seems more broken providing more surface area. Additionally, the increase in ash content before and after gasification is clearly observable in the images. As mentioned earlier, raw coal has around 5 percent ash content reported by the TGA experiment. This percentage has increased to 13 percent for gasified samples and can be seen in the images as lighter spots.
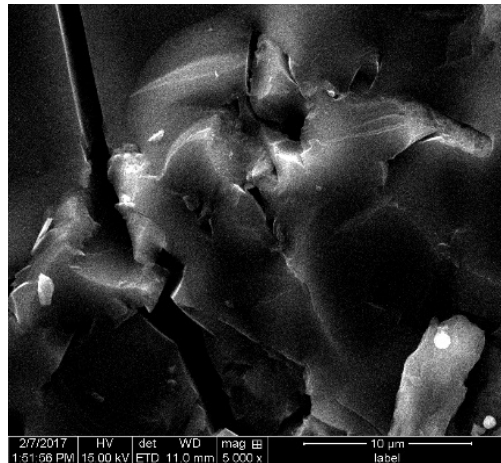
Raw Coal
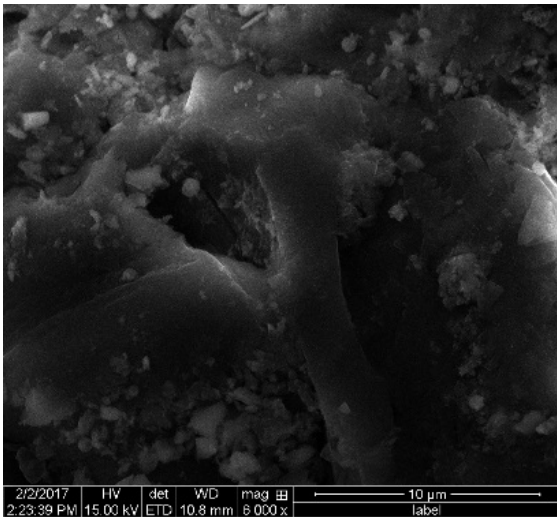
Sample 6
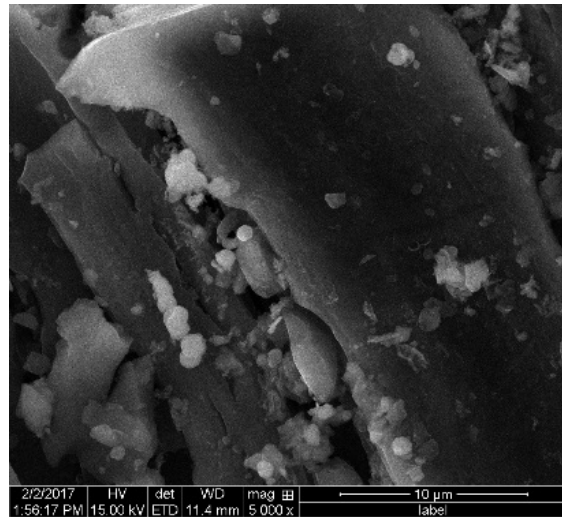
Sample 5
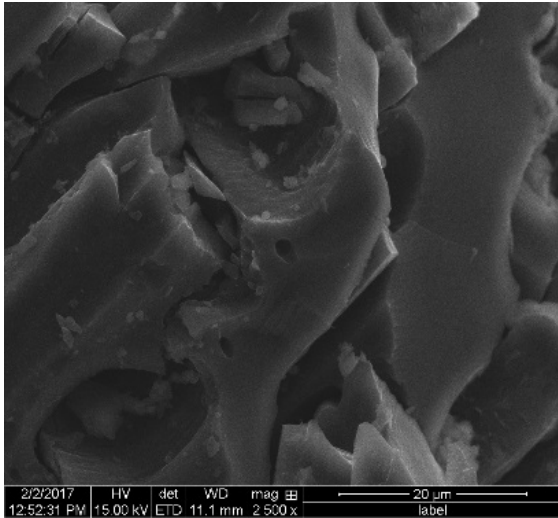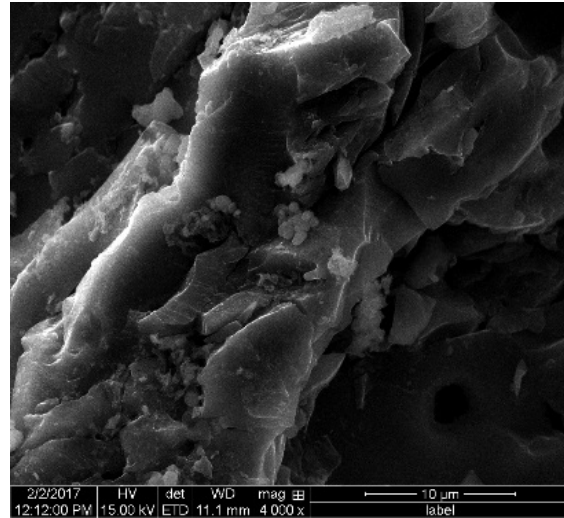
Sample 2   Sample 1
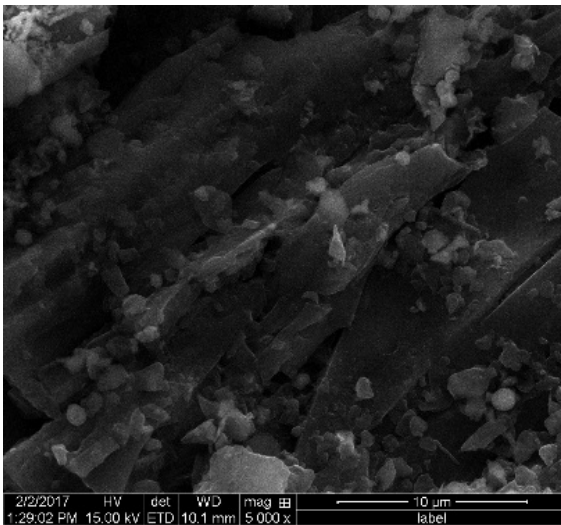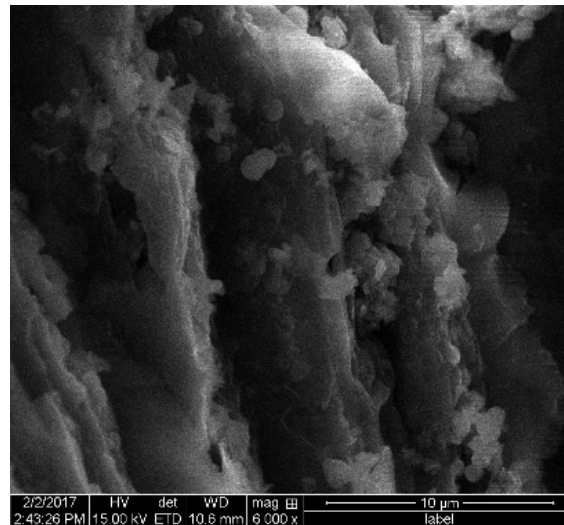
Sample 4   Sample 3

Figure 38 Scanning electron microscopy images of coal samples

Bigger magnifications of two of the samples are presented in figure 38 along with the raw coal image. It is openly observable from these images how fractures and pores are developed after gasification. Pores are more like a tube and cylinder type in both samples. There are fairly large pores in Sample 2 (considering 100 micrometer scale at the bottom of the picture) that probably weren't counted by the CO_2 analyzer test.

Raw Coal Particle   **Sample 2**   **Sample 4**
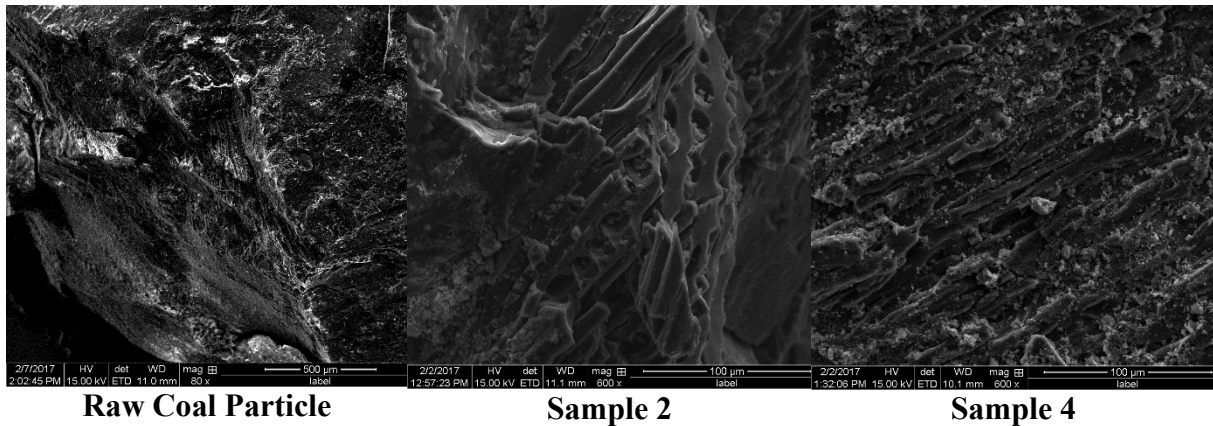
Figure 39 *larger scale raw coal image comparisons with gasified coal*

4.8   Practical application of the UCG-CCS

If the typical proximate analysis of a raw sub-bituminous Canadian coal presented in grams is

considered as follow:

Moisture Content	Volatile Content	Ash Content	Fixed Carbon Content	Sum
6.5	32.4	5.2	55.9	100

The average proximate analysis of the gasified coal after the gasification process would be:

Moisture Content	Volatile Content	Ash Content	Fixed Carbon Content	Sum
1.3	11.8	5.2	24.2	42.6

Incorporating the raw coal density and the density of liquid CO_2, available void volume after

gasification and the maximum possible storage capacity of the post-UCG gasified coal can be

obtained. The corresponding calculations are brought in Table 18.

Table 18 *Practical CO_2 adsorption capacity of the UCG site calculation*

gasified coal mass (gr)	57.4
Row coal density (g/cc)	1.5

available void volume (cc)	38.3
Liquid CO_2 density (gr/c)	1.56
maximum possible CO_2 adsorption (gr)	59.7
maximum CO_2 /gasified coal (gr/gr)	1.4

According to Figures 33 and 37, the average maximum adsorption capacities of the samples are 2.5 mmole/gr and 12 mmole/gr for subcritical and supercritical pressures respectively. If multiplying these adsorption values by the molecular weight of CO_2, grams of CO_2 adsorbed per gram of gasified coal sample is obtained.

Table 19 Maximum CO_2 adsorption capacities of gasified samples

	mmole/gr	gr/gr
super critical adsorption	12	0.528
subcritical adsorption	2.5	0.11

It can be seen from Table 19 that per 1 gram of gasified coal, 0.11 and 0.528 grams of CO_2 can be adsorbed at subcritical and supercritical pressure conditions respectively. These adsorption amounts are still far less than the available void volume in gasified coal (calculated in Table 18) which could theoretically accommodate 1.4 grams of CO2.

Chapter 5

5 Conclusions and future works

The main purpose of this thesis was to estimate the adsorption capacities of gasified coal from the UCG experiments and to understand the relationship between their capacities and physical properties. The experiments were conducted to better understand the storage capability of post-UCG sites for CO_2 capturing and storage fulfillment. The adsorption capacity measurement of the samples were performed using a volumetric adsorption apparatus at 45.5 ºC and pressures from 500 Psia to 1500 Psia. The temperature was fixed at 45.5 ºC to represent the abandoned UCG sites' temperature, and as for the pressures selection, they were chosen in such a way that covers both subcritical and supercritical pressures of CO_2. The gasified samples were taken from the UCG experiment, which was conducted at the University of Alberta. Furthermore, various characterization methods were adopted to correlate the adsorption capacity of the samples to their physical and chemical properties. Samples were grouped into their regions; Region 1 includes samples that were closer to the ignition channel in the UCG, and Region 2 has the samples that were farther away. Proximate and ultimate analysis, petrographic analysis, surface area determination, pore size distribution, and surface morphology through SEM experiments are the techniques used for coal characterization in this study.

According to the results of this study in chapter 4, a summary of the findings are as follows:

The gasification process has converted about 48 to 65 percent of the fixed carbon in the coal to syngas. This was observed through proximate analysis of the samples by calculating the conversion ratio of the ash content in coal. It was also understood that the adsorption process

of CO_2 on coal is a physical adsorption (physisorption) by the comparison of the DTG and TGA graphs of the samples before and after the adsorption process.

Surface area and pore volume of the samples have increased more than two times as a result of gasification. This change was more noticeable in the samples of Region 2 which were farther from the ignition channel. Moreover, the adsorption capacities of the samples increased linearly as their pore volume and surface area increased. The results of the raw and gasified coals were compared with the result of the ash experiment. It was understood that the ash remaining from the gasification process has insignificant adsorption capacity and cannot accommodate CO_2 molecules on its surface despite the pressure force.

According to the pore size distribution (PSD) curves of the samples, micropores mostly with the dimeter of 1.5 nanometers contributed effectively to the surface area of the samples. This contribution was observed through CO_2 surface analyzer tests, which could only capture micropores in the case of this study (Adsorption of CO_2 on coal). Nitrogen surface analyzer tests were also conducted to capture the surface area of the larger pores in the samples. However, the total contribution of the mesopores in the samples obtained from the nitrogen tests was minimal.

Adsorption capacities of the samples increased steadily as the pressure increased in the volumetric adsorption apparatus. The same behavior was observed for the supercritical pressure ranges, but with a sharper slope. Sample 4 and Sample 5 showed the lowest adsorption isotherms. These samples were located at the bottom of Region 1 and lateral layer of Region 2 respectively. According to the CO_2 surface analyzer tests, these samples also had the lowest pore volume, surface area, and atmospheric adsorption isotherms.

The amount of adsorbed gas on coal increases as time passes until reaching a plateau. For experimental purposes, lower wait-time can be considered followed by extrapolation of the results.

The SEM images of the raw and gasified coal show that the gasified samples have a coarser surface caused by pore development, and fracturing during gasification.

Future Works

Coals are known to swell when CO_2 adsorbs on their surface (93) and the swelling of the coal was not considered in this research. For more reliable results, it is important to consider the swelling factor in adsorption measurements. It is also mentioned in the literature that the adsorption of CO_2 on coal, causes deformation of the coal structure and it is beneficial to consider the effect of pore expansion after the pressure is applied for sequestration, to more accurately estimate the capacity of the formation (94).

References

1. Charles D. Keeling, Timothy P. Whorf. The 1,800-Year Oceanic Tidal Cycle: A Possible Cause of Rapid Climate Change. Proceedings of the National Academy of Sciences of the United States of America. 2000 Apr 11,;97(8):3814-9.

2. Online CO2 Emission [Internet].; 2016 [updated Nov 8,;]. Available from: http://www.co2.earth/.

3. Lamb GH. Underground Coal Gasification. Park Ridge, NJ : Noyes Data Corporation; 1977.

4. Carbon sequestration science and technology. 1999.

5. Roddy DJ, Younger PL. Underground coal gasification with CCS: a pathway to de-carbonising industry. Energy & Environmental Science. 2010 Jan 1,;3(4):400-7.

6. J.Q. Shi, S. Durucan. CO2 Storage in Deep Un-minable Coal Seams. 2005;60.

7. Goodman AL, Campus LM, Schroeder KT. Direct Evidence of Carbon Dioxide Sorption on Argonne Premium Coals Using Attenuated Total Reflectance Fourier Transform Infrared Spectroscopy. Energy Fuels. 2005;19(2):471-6.

8. Kwon S, Fan M, DaCosta HFM, Russell AG, Berchtold KA, Dubey MK. Chapter 10 - CO2 Sorption. In: Bell DA, Towler BF, , Fan M, editors. Coal Gasification and Its Applications. Boston: William Andrew Publishing; 2011. p. 293-339.

9. Chemistry international. Research Triangle Park, NC: IUPAC; .

10. Ramasamy S, Sripada PP, Khan MM, Tian S, Trivedi J, Gupta R. Adsorption Behavior of CO2 in Coal and Coal Char. Energy Fuels. 2014;28(8):5241-51.

11. Abunowara M, Bustam MA, Sufian S, Eldemerdash U. Description of Carbon Dioxide Adsorption and Desorption onto Malaysian Coals under Subcritical Condition. Procedia Engineering. 2016;148:600-8.

12. Krooss BM, van Bergen F, Gensterblum Y, Siemons N, Pagnier HJM, David P. High-pressure methane and carbon dioxide adsorption on dry and moisture-equilibrated Pennsylvanian coals. International Journal of Coal Geology. 2002;51(2):69-92.

13. Bae J, Bhatia SK. High-Pressure Adsorption of Methane and Carbon Dioxide on Coal. Energy Fuels. 2006;20(6):2599-607.

14. Sripada PP, Khan MM, Ramasamy S, Kanneganti V, Trivedi J, Gupta R. Comparison of CO2 Storage Potential in Pyrolysed Coal Char of different Coal Ranks. In: Gas Injection for Disposal and Enhanced Recovery. John Wiley & Sons, Inc.; 2014. p. 293-304.

15. Coal and steel. UK: Aspermont Media UK; 2001 Nov 30,. Report No.: 337.

16. Kempka T, Fernández-Steeger T, Li D, Schulten M, Schlüter R, Krooss BM. Carbon Dioxide Sorption Capacities of Coal Gasification Residues. Environ Sci Technol. 2011;45(4):1719-23.

17. D. P. Creedy, K Garner. Review of underground coal gasification technological advancement. London [u.a.]: Elsevier Applied Science; 1989.

18. Ruprecht P, Schäfer W, Wallace P. A computer model of entrained coal gasification. Fuel. 1988;67(6):739-42.

19. Younger PL. Hydrogeological and Geo-mechanical Aspects of Underground Coal Gasification and its Direct Coupling to Carbon Capture and Storage. Mine Water and the Environment. 2011;30(2):127-40.

20. Nakaten N, Islam R, Kempka T. Underground Coal Gasification with Extended CO2 Utilization - An Economic and Carbon Neutral Approach to Tackle Energy and Fertilizer Supply Shortages in Bangladesh. Energy Procedia. 2014;63:8036-43.

21. Chadwick A. Best practice for the storage of CO2 in saline aquifers - observations and guidelines from the SACS and CO2 store projects. ; 2008.

22. Sarhosis V, Yang D, Sheng Y, Kempka T. Coupled Hydro-thermal Analysis of Underground Coal Gasification Reactor Cool Down for Subsequent CO2 Storage. Energy Procedia. 2013;40:428-36.

23. Yang D, Koukouzas N, Green M, Sheng Y. Recent development on underground coal gasification and subsequent CO2 storage. Journal of the Energy Institute. 2016;89(4):469-84.

24. Gregg S.J., Sing K S W. Adsorption, Surface Area and Porosity. second ed.

25. Adsorption by carbons / edited by Eduardo J. Bottani and Juan M.D. Tascón. 1st ed ed. Amsterdam: Elsevier; 2008.

26. Bandosz TJ. Gas Adsorption Equilibria: Experimental Methods and Adsorptive Isotherms By Jürgen U. Keller and Reiner Staudt (Universität Siegen). Springer: New York. 2005. xiv + 442 pp. $139.00. ISBN 0-387-23597-3. J Am Chem Soc. 2005;127(20):7655-6.

27. Hubbard A. Adsorption: Theory, Modeling and Analysis. Edited by József Tóth. Elsevier Inc; 2003.

28. Adsorbents Fundamentals and Applications.

29. Suzuki M. Adsorption engineering. Tokyo u.a: Kodansha u.a; 1990.

30. Duong D. Do. Adsorption analysis. GB: Imperial College Press; 1998.

31. Stephen Brunauer, P. H. Emmett, Edward Teller. Adsorption of Gases in Multimolecular Layers. 1938;60.

32. Dubinin MM. The Potential Theory of Adsorption of Gases and Vapors for Adsorbents with Energetically Nonuniform Surfaces. Chemical Reviews. 1960 Apr 1,;60(2):235-41.

33. Burwell RL. Manual of Symbols and Terminology for Physicochemical Quantities and Units-Appendix II. Elsevier Science; 2013.

34. B. McEnaney, T J . Mays. Porosity in Carbons and Graphites.

35. J.R. Levine. Exploring coalbed methane reservoir. Rueil-Malmaison: 1993.

36. Günter Tiess, Tapan Majumder, Peter Cameron, editors. Encyclopedia of mineral and energy policy Springer Berlin Heidelberg; 2015.

37. McGlashan ML. Manual of symbols and terminology for physicochemical quantities and units. 2. impr. ed. London: Butterworths; 1971.

38. Alexeev AD. Physics of Coal and Mining Processes. 1st ed. London: CRC Press; 2016.

39. Fejgin LA, Svergun DI. Structure analysis by small-angle X-ray and neutron scattering. New York: Plenum Pr; 1987.

40. Marsh H, Rodríguez-Reinoso F. Activated carbon. 1. ed. ed. Amsterdam [u.a.]: Elsevier; 2006.

41. Bakhmutov VI. NMR Spectroscopy in Liquids and Solids. Oakville: CRC Press; 2015.

42. Zhang Y, Bao N, Huang Z, Xue B, Gao Y. Research on Relationship Between Porosity of Coal, Amount of Air Leakage and Gradient of Wind Pressure. Procedia Engineering. 2012;45:774-9.

43. Rodrigues CF, Lemos de Sousa, M J. The measurement of coal porosity with different gases. International Journal of Coal Geology. 2002;48(3–4):245-51.

44. Apostolos Kantzas, Jonathan Bryan, Saeed Taheri. Fundamentals of Fluid Flow in Porous Media. Calgary: .

45. Do DD, Do HD. Pore characterization of carbonaceous materials by DFT and GCMC simulations: a review. Adsorption Science & Technology. 2003;21(5):389-423.

46. Ryu Z, Zheng J, Wang M, Zhang B. Characterization of pore size distributions on carbonaceous adsorbents by DFT. Carbon. 1999;37(8):1257-64.

47. Sircar S. Gibbsian Surface Excess for Gas AdsorptionRevisited. Ind Eng Chem Res. 1999;38(10):3670-82.

48. Gravimetric Sorption Analysis [Internet]. [cited January 18, 2017].

49. Perera MSA, Ranjith PG, Choi SK, Airey D, Weniger P. Estimation of Gas Adsorption Capacity in Coal: A Review and an Analytical Study. International Journal of Coal Preparation and Utilization. 2012;32(1):25-55.

50. Crosdale PJ, Beamish BB, Valix M. Coalbed methane sorption related to coal composition. International Journal of Coal Geology. 1998;35(1–4):147-58.

51. Wang, Xingjin, School of Biological, Earth & Environmental Science, UNSW. Influence of coal quality factors on seam permeability associated with coalbed methane production [dissertation]. ; 2007.

52. Bustin RM, Clarkson CR. Geological controls on coalbed methane reservoir capacity and gas content. International Journal of Coal Geology. 1998;38(1–2):3-26.

53. Harris LA, Yust CS. Transmission electron microscope observations of porosity in coal. Fuel. 1976;55(3):233-6.

54. P. D. Gamson, B B Beamish, editor. Coal type, microstructure, and gas flow behavior of Bowen basin coals. Townsville: Coalbed methane symposium; 1992.

55. Crosdale PJ, Moore TA, Mares TE. Influence of moisture content and temperature on methane adsorption isotherm analysis for coals from a low-rank, biogenically-sourced gas reservoir. International Journal of Coal Geology. 2008;76(1):166-74.

56. Gürdal G, Yalçın MN. Pore volume and surface area of the Carboniferous coals from the Zonguldak basin (NW Turkey) and their variations with rank and maceral composition. International Journal of Coal Geology. 2001;48(1–2):133-44.

57. Wang, Xingjin, School of Biological, Earth & Environmental Science, UNSW. Influence of coal quality factors on seam permeability associated with coalbed methane production [dissertation]. ; 2007.

58. Saghafi A, Faiz M, Roberts D. CO2 storage and gas diffusivity properties of coals from Sydney Basin, Australia. International Journal of Coal Geology. 2007;70(1–3):240-54.

59. Mavor MJ, Close JC. Western cretaceous coal seam project formation evaluation of coalbed methane wells. Topical report, January 1988-December 1991. United States: 1991 Nov 15.

60. Rice, D. D., B. E. Law, and J. L. Clayton. Coal bed gas: An undeveloped resource. In The Future of Energy Gases. U.S. geological survey professional paper. 1995;1570:389-404.

61. Clarkson CR, Bustin RM. Binary gas adsorption/desorption isotherms: effect of moisture and coal composition upon carbon dioxide selectivity over methane. International Journal of Coal Geology. 2000;42(4):241-71.

62. Laxminarayana C, Crosdale PJ. Role of coal type and rank on methane sorption characteristics of Bowen Basin, Australia coals. International Journal of Coal Geology. 1999;40(4):309-25.

63. Zhang L, Aziz N, Ren TX, Wang Z. Influence of Temperature on Coal Sorption Characteristics and the Theory of Coal Surface Free Energy. Procedia Engineering. 2011;26:1430-9.

64. Gürdal G, Yalçın MN. Gas adsorption capacity of Carboniferous coals in the Zonguldak basin (NW Turkey) and its controlling factors. Fuel. 2000;79(15):1913-24.

65. Lamberson MN, Bustin RM. Coalbed methane characteristics of Gates Formation coals, northeastern British Columbia; effect of maceral composition. AAPG Bulletin. 1993 Dec 1,;77(12):2062.

66. Faiz M, Saghafi A, Sherwood N, Wang I. The influence of petrological properties and burial history on coal seam methane reservoir characterization, Sydney Basin, Australia. International Journal of Coal Geology. 2007;70(1–3):193-208.

67. Moffat, D. H., and K. E. Weale. Sorption by coal of methane at high pressures. Fuel. 1955;34:449-62.

68. Levy JH, Day SJ, Killingley JS. Methane capacities of Bowen Basin coals related to coal properties. Fuel. 1997;76(9):813-9.

69. White CM, Smith DH, Jones KL, Goodman AL, Jikich SA, LaCount RB, et al. Sequestration of Carbon Dioxide in Coal with Enhanced Coalbed Methane Recovery A Review. Energy Fuels. 2005;19(3):659-724.

70. Chen S, Jin L, Chen X. The effect and prediction of temperature on adsorption capability of coal/CH4. Procedia Engineering. 2011;26:126-31.

71. Yang RT, Saunders JT. Adsorption of gases on coals and heat-treated coals at elevated temperature and pressure. Fuel. 1985;64(5):616-20.

72. Mazzotti M, Pini R, Storti G. Enhanced coalbed methane recovery. The Journal of Supercritical Fluids. 2009;47(3):619-27.

73. Durucan S, Edwards JS. The effects of stress and fracturing on permeability of coal. Mining Science and Technology. 1986;3(3):205-16.

74. Karacan CÖ. Heterogeneous Sorption and Swelling in a Confined and Stressed Coal during CO_2 Injection. Energy Fuels. 2003;17(6):1595-608.

75. Xue Z, Ohsumi T. Coal matrix swelling caused by adsorption of carbon dioxide and its impact on permeability. In: Greenhouse Gas Control Technologies. Elsevier Science Ltd; 2005. p. 2253-6.

76. Kan Yang, Xiancai Lu, Yangzheng Lin, Alexander V. Neimark. Effects of CO_2 adsorption on coal deformation during geological sequestration. Journal of Geophysical Research. Solid Earth. 2011 Aug 1,;116(8).

77. Saxena SC. Devolatilization and combustion characteristics of coal particles. Progress in Energy and Combustion Science. 1990;16(1):55-94.

78. Peter F. Nelson, Ian W. Smith, Ralph J. Tyler. Pyrolysis of Coal at High Temperatures. Energy & Fuels. 1988;2.

79. Balek V, de Koranyi A. Diagnostics of structural alterations in coal: Porosity changes with pyrolysis temperature. Fuel. 1990;69(12):1502-6.

80. Walker PL. Pore system in coal chars. Implications for diffusion parameters and gasification. Fuel. 1980;59(11):809-10.

81. Wei De Jiang, Lee I, Yang RYK. Microstructural variations of lignite, subbituminous and bituminous coals and their high temperature chars. Fuel Process Technol. 1988;18(1):11-23.

82. Razouk RI, Saleeb FZ, Youssef AM. The effect of thermal treatment on the surface area of coal. Carbon. 1968;6(3):325-31.

83. Toda Y, Hatami M, Toyoda S, Yoshida Y, Honda H. Fine structure of carbonized coals. Carbon. 1970;8(4):565-71.

84. Miura S, Silveston PL. Change of pore properties during carbonization of coking coal. Carbon. 1980;18(2):93-108.

85. Feng B, Bhatia SK. Variation of the pore structure of coal chars during gasification. Carbon. 2003;41(3):507-23.

86. Roberts DG, Harris DJ. Char gasification in mixtures of CO_2 and H_2O: Competition and inhibition. Fuel. 2007;86(17–18):2672-8.

87. Batchelder HR, Busche RM, Armstrong WP. Kinetics of Coal Gasification: Proposed Mechanism of Gasification; Development of Reaction Rate Equations; Development of Heat Transfer Equations and Method of Calculation; Calculated Relation between Gasifier Yields and Process Variables. Ind Eng Chem. 1953;45(9):1856-78.

88. Span R, Wagner W. A New Equation of State for Carbon Dioxide Covering the Fluid Region from the Triple-Point Temperature to 1100 K at Pressures up to 800 MPa. Journal of Physical and Chemical Reference Data. 1996 Nov;25(6):1509-96.

89. Gold V. Compendium of chemical terminology. Reprint ed. Oxford [u. a.]: Blackwell; 1992.

90. Diessel CFK. Coal-bearing depositional systems. Berlin [u.a.]: Springer; 1992.

91. Lee M, Park M, Kim HY, Park S. Effects of Microporosity and Surface Chemistry on Separation Performances of N-Containing Pitch-Based Activated Carbons for CO_2/N_2 Binary Mixture. Scientific Reports. 2016;6:23224.

92. An F, Cheng Y, Wu D, Wang L. The effect of small micropores on methane adsorption of coals from Northern China. Adsorption. 2013;19(1):83-90.

93. Schieferstein E, Möller A, Laggner P, Matysik J, Schlüter R, Hemza P. Investigation of adsorption and swelling behaviour of coal to determine the feasibility of CO_2 sequestration and CH_4 production enhancement (Coalswad). . 2013;25895.

94. Yang K, Lu X, Lin Y, Neimark AV. Effects of CO_2 adsorption on coal deformation during geological sequestration. J Geophys Res. 2011;116:n/a.